


## Shot-noise cojumps: Exact simulation and option pricing

Yan Qu<sup>a</sup>, Angelos Dassios<sup>b</sup> and Hongbiao Zhao<sup>c,d</sup> 

<sup>a</sup>Beijing University of Posts and Telecommunications, Beijing, China; <sup>b</sup>London School of Economics, London, United Kingdom; <sup>c</sup>Shanghai University of Finance and Economics, Shanghai, China; <sup>d</sup>Shanghai Institute of International Finance and Economics, Shanghai, China

### ABSTRACT

We consider a parsimonious framework of jump-diffusion models for price dynamics with stochastic price volatilities and stochastic jump intensities in continuous time. They account for conditional heteroscedasticity and also incorporate key features appearing in financial time series of price volatilities and jump intensities, such as persistence of contemporaneous jumps (*cojumps*), mean reversion and feedback effects. More precisely, the stochastic variance and stochastic intensity are jointly modelled by a generalised bivariate shot-noise process sharing common jump arrivals with any non-negative jump-size distributions. This framework covers many classical and important models in the literature. The main contribution of this paper is that, we develop a very efficient scheme for its exact simulation based on *perfect decomposition* where neither numerical inversion nor acceptance/rejection scheme is required, which means that it is not only accurate but also the efficiency would not be sensitive to the parameter choice. Extensive numerical implementations and tests are reported to demonstrate the accuracy and effectiveness of this scheme. Our algorithm substantially outperforms the classical discretisation scheme. Moreover, we unbiasedly estimate the prices of discrete-barrier European options to show the applicability and flexibility of our algorithms.

### ARTICLE HISTORY

Received 30 January 2020  
Accepted 8 May 2022

### KEYWORDS

Exact simulation; Monte Carlo simulation; jump-diffusion models; stochastic volatility models; shot-noise process; contemporaneous jumps; cojumps; shot-noise cojumps; option pricing; systemic risk

### MATHEMATICS SUBJECT CLASSIFICATION (2010):

Primary: 91G60; 91B25;  
Secondary: 65C05; 60H35;  
60G17; 91G20

### JEL CLASSIFICATION:

C15; G13; C63

## 1. Introduction

Existence of discontinuities or jumps in the asset price (or return), its volatility and even its jump intensity in the market have been extensively studied in the literature. Incorporating jumps in asset prices for option pricing was already presented in the seminal work by Merton (1976). Similarly, price volatility may also exhibit jumps, and the empirical importance of jumps in volatility implied from the option market as well as in the high-frequency data has been well documented in Bakshi et al. (1997); Bates (2000); Pan (2002); Todorov and Tauchen (2011). Even though both types of jumps have been included, the resulting models still can not fully capture the real time series which have been observed in the financial market. Adding jumps in its jump intensity becomes a natural extension, see the more general models of *affine framework* developed by Duffie et al. (2000, 2003).

Recent evidences further reveal that these jumps in prices (or returns), price volatilities and jump intensities may occur simultaneously, especially when nowadays large high-frequency data are

available and associated econometrical methods for detecting jumps have been developed. More precisely, there are mainly two types of *contemporaneous jumps*, or *cojumps* for an asset: There are contemporaneous jumps (i.e. *price-volatility cojumps*) in the asset price (or return) and its volatility that may present “leverage effects”, see Eraker et al. (2003); Eraker (2004); Broadie et al. (2007); Jacod and Todorov (2010); Todorov and Tauchen (2011); Bandi and Renò (2012, 2016); Jacod et al. (2012, 2017); Andersen et al. (2015a, 2015b); Fulop et al. (2015) and (Aït-Sahalia & Jacod, 2014, Sec.14.2). For example, Todorov and Tauchen (2011) provided empirical evidence from the high-frequency data of the close-to-maturity options written on the stock market index that, the volatility jumps and market price jumps occur in most of the same time and exhibit high negative dependency. In addition, as shocks to the price dynamics are likely to propagate over time, there are contemporaneous jumps (i.e. *price-intensity cojumps*) in the asset price (or return) and its jump intensity that may present “feedback effects” or “contagion effects”, see Aït-Sahalia et al. (2014, 2015); Xiu (2014); Fulop et al.

(2015); Ait-Sahalia and Hurd (2015); Carr and Wu (2017); Boswijk et al. (2018); Corradi et al. (2018); Dungey et al. (2018); Nyström and Zhang (2021). This type of price-intensity cojumps has become more important since the global financial crisis of 2007–2008. Overall, the concurrence mechanism of jumps makes diversification less effective and contributes to another layer of systemic risk to the market. Therefore, modelling the dynamics of these cojumps is of paramount importance for risk management, asset pricing, trading, as well as to study the unanticipated transmission of shocks, explain risk premia and understand the behaviors of investors and markets.

Both the volatility process and jump intensity process are apparently not observable. Volatility is directly related to the rate of information flow in the market (Ross, 1989), and information often comes in packets or clusters randomly. Therefore, stochastic volatility presents some key features that often appear in the financial time series, such as mean reversion and *volatility clustering* (i.e. the tendency of large changes in asset prices, either positive or negative, to be followed by large changes, and small changes to be followed by small changes). As surveyed by (Shephard, 2005, p.11) and Broadie et al. (2007), the earliest model in the literature that incorporates these elements in the volatility process is probably the so-called *shot-noise SV model* used by Bookstaber and Pomerantz (1989). It is a simple mean-reverting pure-jump model for volatility dynamics that could reflect the digestion of information after events are sequentially and discretely revealed to the public in the market (Peng & Xiong, 2003). It arises naturally in a financial market with stochastic information flows, and the process of digesting information by investors has a rate that changes endogenously through time. Very recent nonparametric evidence from Todorov et al. (2014) also suggests that volatility may evolve only through jumps. Meanwhile, jump intensity acts similarly as volatility and shares many common features. Therefore, we adopt a generalised bivariate *shot-noise process* (Cox & Isham, 1980, p.88) with two types of cojumps for modelling the joint evolution of volatility and intensity<sup>1</sup>. It is a *shot-noise stochastic volatility (SV) model*<sup>2</sup>, which accounts for conditional heteroscedasticity (i.e. time-varying volatility), and incorporate basic and important features appearing in financial time series of volatility, such as persistence of contemporaneous jumps (shocks) and mean reversion. On the other hand, it is a *shot-noise stochastic intensity model* that can also capture “feedback effects” by adding price-intensity cojumps. All together, it forms a class of

parsimonious and highly analytically tractable pure-jump stochastic volatility models in continuous time.

Due to the importance of the role that these types of cojumps play in financial markets and the high volume of recent literature on this issue, it would be useful to develop a very efficient, accurate and easy-to-use numerical scheme of sampling them for practical implementation. In this paper, we aim to introduce this parsimonious framework of SV models which incorporate both types of cojumps meanwhile the resulting price processes still can be exactly and quickly simulated without bias, so that cojumps can be very accurately and efficiently generated in normal computers for asset pricing (e.g. options), risk management (e.g. stress tests, back tests for trading strategies and portfolio management), or for simulation-based study and testing for some newly developed statistical or econometric methods. Conventional simulation methods (such as Euler scheme) widely adopted both in industry and literature for stochastic volatility models are mainly based on discretising the underlying processes and simulating approximately by *time discretisation* (Glasserman, 2003). Although simple and generally applicable, they introduce bias into simulation-based estimations. In contrast, *exact simulation* for stochastic volatility models has the primary advantage of generating sample paths according to the process law exactly, and it is especially useful for unbiasedly estimating option prices. It is an interesting and challenging problem which has attracted many researchers recently. Beskos and Roberts (2005) developed an exact simulation algorithm based on the *acceptance/rejection* (A/R) scheme for one-dimensional state-dependent diffusions. It was then extended by Chen and Huang (2013) to exactly simulate a more general class of diffusions via a *localisation* technique. Broadie and Kaya (2006) designed an exact simulation algorithm for the classical Heston (1993)’s CIR SV model. Recently, it has been further extended by Baldeaux (2012) for the 3/2 SV model, Grasselli (2017) for the 4/2 SV model, Cai et al. (2017) for the SABR model, Kang et al. (2017) for the Wishart SV model, and Li and Wu (2019) for the Ornstein–Uhlenbeck SV model. However, all of them heavily rely on the numerical inversion scheme for Laplace (Fourier) transforms, and it is well known that it involves truncation and discretisation errors. In contrast, we develop algorithms for *exact simulation* without any numerical inversion or truncation. Our key methodology for simulation design is based on the exact *distributional decomposition*<sup>3</sup> for the underlying stochastic processes. The key advantage of this approach is that it does not involve numerical inversion

procedure. In addition, for this shot-noise cojump framework in particular here, remarkably, we even discover a *perfect decomposition* such that the process can be decomposed into simple random variables which can be exactly simulated directly without any A/R scheme. This means that it is not only accurate but also the efficiency would not be sensitive to the parameter choice. As illustrated in later sections, our algorithm is extremely fast, and substantially outperforms the classical discretisation scheme. Moreover, our scheme allows very flexible distributions and their dependency structure among these sizes of cojumps.

The paper is organised as follows: Section 2 sets up the model framework of shot-noise cojumps. The associated exact simulation algorithms with relevant distributional properties are developed in Section 3. In Section 4, we implement, validate our algorithms, and offer an application to option pricing with extensive numerical experiments; comparisons with the classical discretisation scheme as well as the analysis of performance sensitivity to parameter choice are also provided. Section 5 draws a brief conclusion for this paper.

## 2. Model Framework of shot-noise cojumps

To simplify the model setup, we assume the risk-free interest rate is fixed and the asset is a stock which pays no dividend. The price dynamics is modelled by a jump-diffusion framework with shot-noise stochastic volatility and stochastic intensity on a filtered probability space  $(\Omega, \mathcal{F}, \mathbb{P})$ . It has contemporaneous and (in)dependent jumps (i.e. cojumps) in price, variance and intensity processes. This is to capture exogenous shocks (e.g. news) simultaneously acting on the price, volatility and intensity processes, which immediately present cojumps with (in)dependent random sizes. Each impact of shocks to the volatility or intensity decays exponentially afterward. In addition, there is a series of contagious cojumps in the price and intensity to capture the “feedback” or “contagion” effects. More precisely, it is specified in Definition 2.1 in general as follows.

**Definition 2.1** (Shot-noise Cojump Framework). The price process  $\{S_t\}_{t \geq 0}$  under the equivalent martingale measure  $\mathbb{Q} \sim \mathbb{P}$  follows a jump-diffusion process characterised by the stochastic differential equations (SDEs)

$$\frac{dS_t}{S_t} = (r - c_t)dt + \sqrt{V_t}dW_t + (e^{J_t} - 1)dN_t + (e^{J_t^*} - 1)dN_t^*, \tag{2.1}$$

$$dV_t = -\delta(V_t - \mu_V)dt + Y_t^V dN_t, \tag{2.2}$$

$$d\lambda_t = -\kappa(\lambda_t - \mu_\lambda)dt + Y_t dN_t + Y_t^* dN_t^*, \tag{2.3}$$

$$c_t = (\mu_S - 1)\varrho + (\mu^* - 1)\lambda_t, \tag{2.4}$$

where

- $r \geq 0$  is the constant of risk-free interest rate;
- $\{W_t\}_{t \geq 0}$  is a standard Brownian motion;
- $V_t$  is the shot-noise *stochastic volatility* (or *instantaneous variance rate*);
- $\delta > 0$  is the constant mean-reversion rate of volatility;
- $\mu_V \geq 0$  is the constant mean-reversion level of volatility;
- $N_t$  is the counting process of **price-volatility-intensity cojumps**, which follows a standard Poisson process of constant intensity  $\bar{\sigma} > 0$  and characterises the price-volatility-intensity cojump arrival times  $\{T_i\}_{i=1,2,\dots}$ , i.e.,  $N \equiv \{T_i\}_{i=1,2,\dots}$ ;
- $N_t^*$  is the counting process<sup>4</sup> of **price-intensity cojumps** with shot-noise stochastic intensity  $\lambda_t$ , which characterises the price-intensity cojump arrival times  $\{T_j^*\}_{j=1,2,\dots}$ , i.e.  $N^* \equiv \{T_j^*\}_{j=1,2,\dots}$ ;
- $\kappa > 0$  is the constant mean-reversion rate of intensity;
- $\mu_\lambda \geq 0$  is the constant mean-reversion level of intensity;
- $\{(J_i, Y_i^V, Y_i)\}_{i=1,2,\dots}$  are the cojump sizes in price, volatility and intensity, respectively, with any joint distribution  $Q(y_1, y_2, y_3)$ ,  $y_1 \in \mathbb{R}, y_2, y_3 \geq 0$ , and the marginal distribution  $H(y), y \geq 0$  for  $Y_i^V$ , where  $J_i := J_{T_i}, Y_i^V := Y_{T_i}^V$  and  $Y_i := Y_{T_i}$ ;
- $\{(J_j^*, Y_j^*)\}_{j=1,2,\dots}$  are another series of cojump sizes in price and intensity, respectively, which are *i.i.d.* following a non-negative distribution with the joint distribution  $Q^*(x_1, x_2)$ ,  $x_1 \in \mathbb{R}, x_2 \geq 0$  where  $J_j^* := J_{T_j}^*$  and  $Y_j^* := Y_{T_j}^*$ ;
- $N_t$  and  $W_t$  are assumed to be independent of each other, and

$$\mu_S := \mathbb{E}[e^{J_i}], \quad \mu^* := \mathbb{E}[e^{J_j^*}], \quad \forall i, j. \tag{2.5}$$

Given the initial volatility level and initial intensity level,  $V_0, \lambda_0 > 0$  (which could be fixed or random), the *shot-noise stochastic volatility* and the *shot-noise stochastic intensity* as characterised by the SDEs (2.2, 2.3) respectively can be explicitly expressed as the solutions of

$$V_t = \mu_V + (V_0 - \mu_V)e^{-\delta t} + \sum_{i=1}^{N_t} Y_i^V e^{-\delta(t-T_i)},$$

$$\lambda_t = \mu_\lambda + (\lambda_0 - \mu_\lambda)e^{-\kappa t} + \sum_{i=1}^{N_t} Y_i e^{-\kappa(t-T_i)} + \sum_{j=1}^{N_t^*} Y_j^* e^{-\kappa(t-T_j^*)}.$$

Exactly simulated sample paths of the asset price  $S_t$  with the underlying stochastic shot-noise volatility  $V_t$  and stochastic shot-noise intensity  $\lambda_t$  using our

newly-developed simulation algorithm (which will be provided later in Algorithm 3.2) for this *shot-noise cojump framework* are plotted in Figure 1 with parameter setting (4.1, 4.2, 4.3) specified later in Section 4.2.

The most flexible setting in this framework is that these cojump sizes can follow any non-negative distributions and even can be dependent on history of the processes or other variables. In addition, we can also incorporate the leverage effect (i.e. negative dependency between the asset price and its volatility) by setting a negative dependence for the sizes of cojumps in the asset price and its volatility.

This shot-noise cojump framework is a parsimonious specification of the general *affine framework* (Duffie et al., 2000, 2003). However, it is comprehensive enough to capture most of fundamental components (such as diffusion and jumps in price, conditional heteroscedasticity, mean-reverting stochastic volatility, stochastic cojumps in price and volatility, leverage effect, stochastic intensity, clustering jumps, contagion effect) as presented from the real financial time series, meanwhile maintaining the underlying models parsimonious and exactly simulatable without numerical inversion and A/R procedure (as demonstrated in the next section). This framework covers many classical and important jump-diffusion models in the literature. Of course, it covers the *Black-Scholes model* (Black & Scholes, 1973) when the volatility and intensity are fixed and there is no any jumps in the price process. If  $J_t^* \equiv 0$ ,  $V_t$  is a fixed positive constant and the jump size  $J_t$  follows a normal distribution, then it reduces to the classical *Merton's jump-diffusion model* (Merton, 1976); if the logarithm of  $J_t$  follows an asymmetric double exponential distribution, then, it reduces to the *Kou's jump-diffusion model* (Kou, 2002). If  $J_t = J_t^* \equiv 0$ , it is a *pure shot-noise SV model*. If  $J_t^* \equiv 0$ , then, it is a shot-noise SV model with contemporaneous price-volatility jumps (*shot-noise SVCJ model*). If  $J_t^* \equiv 0$ ,  $\mu_V = 0$  and the jump size  $Y_t^V$  follows an exponential distribution, then, it is a *gamma-OU SV model* (Barndorff-Nielsen & Shephard, 2001a, 2002; Roberts et al., 2004)<sup>5</sup>. If  $J_t \equiv 0$  and the volatility is fixed, then, it reduces to the *Hawkes' jump-diffusion model* (Ait-Sahalia et al., 2015). Our framework is also similar to (but different from) the very recent option-pricing model of Andersen et al. (2015b) but with a simpler parametrisation. However, we focus on the development of simulation algorithm rather than empirical analysis.

### 3. Exact simulation

In this section, we develop a highly efficient scheme of exact simulation for this shot-noise cojump

framework. We denote the Laplace transform, mean, *integrated volatility*, *integrated intensity* and *integrated compensator* respectively by

$$\begin{aligned} \hat{h}(u) &:= \int_0^\infty e^{-uy} dH(y), & \mu_H &:= \int_0^\infty y dH(y); \\ I_t &:= \int_0^t V_s ds, & I_0 &= 0; & \Lambda_t &:= \int_0^t \lambda_s ds, \\ \Lambda_0 &= 0; & C_t &:= \int_0^t c_s ds, & C_0 &= 0, \end{aligned}$$

where  $c_t$  is the compensator of cojumps in the price process. Obviously, we have the simple connection between the integrated compensator process  $C_t$  and the integrated intensity process  $\Lambda_t$ ,

$$C_t = (\mu_S - 1)qt + (\mu^* - 1)\Lambda_t. \quad (3.1)$$

By taking the risk-free bond (with risk-free interest rate  $r$ ) as the numeraire, the discounted price process  $\{e^{-rt}S_t\}_{t \geq 0}$  has to be a  $\mathbb{Q}$ -martingale in order to eliminate arbitrage opportunity. Obviously, with the compensator  $c_t$  specified by (2.4), for any time  $t > 0$ , we have

$$\mathbb{E}[S_t|S_0] = S_0 e^{rt}. \quad (3.2)$$

For conciseness, in the sequel, we focus on the cases with the mean-reversion level  $\mu_V = 0$ , as it is trivial to extend to the cases with  $\mu_V > 0$  by simply changing variable  $V_t$  by  $V_t - \mu_V$ .

#### 3.1. Distributional properties

A key difference from many other SV models in the literature is that, there is no diffusion in volatility or intensity in our shot-noise cojump framework. This simplification makes it more analytically tractable than most other SV models in the literature. Remarkably, it has nice distributional properties and even allows perfect decomposition for the underlying transition processes within any given time period  $[T, T + \tau]$ ,  $\tau \in \mathbb{R}^+$ .

The point increments of two types  $N_t$  and  $N_t^*$  within the time period  $[T, T + \tau]$  are respectively denoted by

$$\Delta N_\tau := N_{T+\tau} - N_T, \quad \Delta N_\tau^* := N_{T+\tau}^* - N_T^*.$$

As specified in Definition 2.1, it is clear that,  $\Delta N_\tau$  follows a Poisson random variable of rate  $qt$ . However,  $\Delta N_\tau^*$  is more complicated, which will be discussed in detail later in Section 3.2. It is well known that,

$$\int_T^{T+\tau} \sqrt{V_s} dW_s \mid I_{T+\tau} - I_T \sim \mathcal{N}(0, I_{T+\tau} - I_T),$$

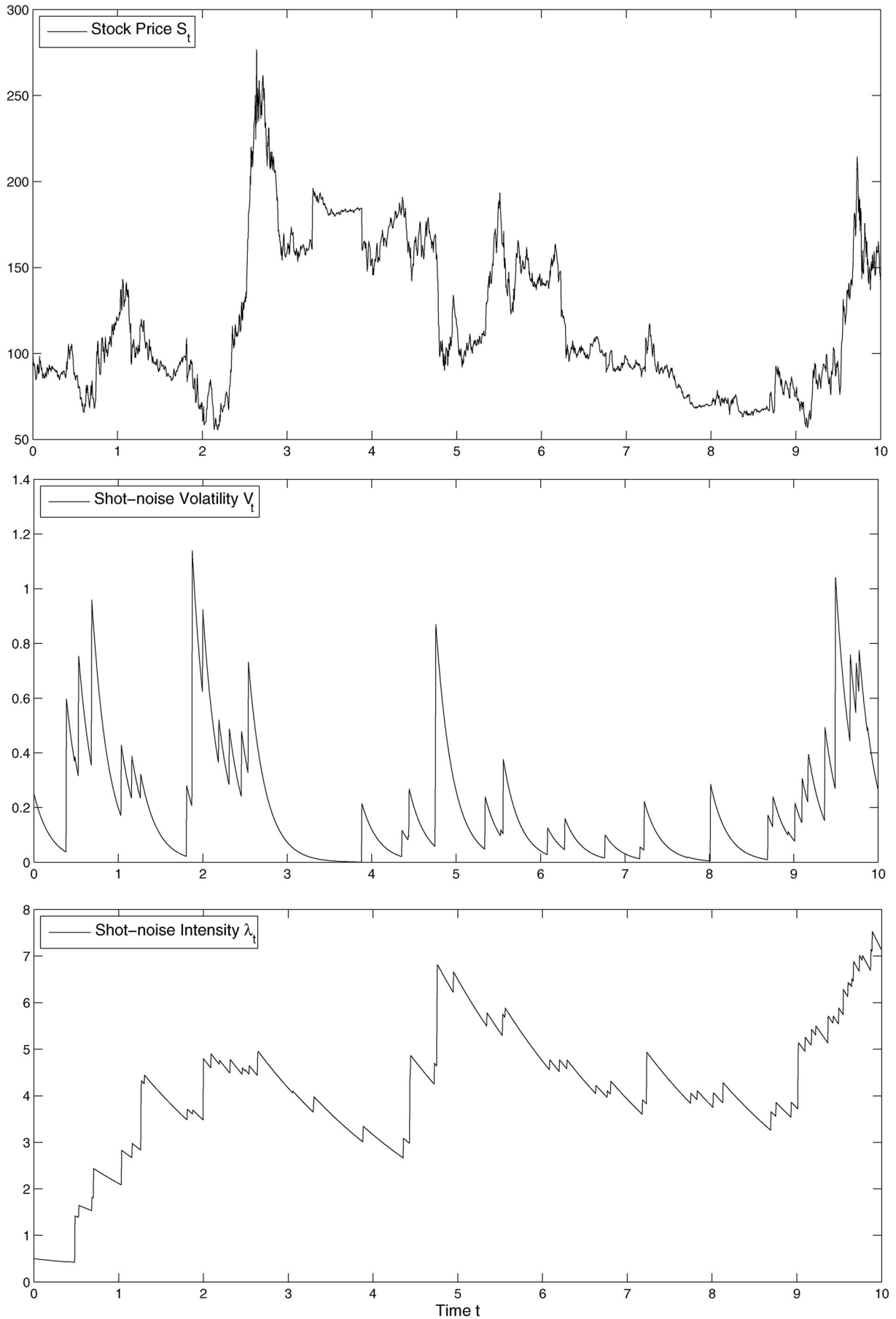


**Figure 1.** Exactly simulated sample paths of asset price  $S_t$ , stochastic shot-noise volatility  $V_t$  and stochastic shot-noise intensity  $\lambda_t$  using our newly-developed simulation scheme (Algorithm 3.2) for the shot-noise cojump model with parameter setting (4.1, 4.2, 4.3) specified later in Section 4.2.

where  $I_{T+\tau} - I_T$  is the *actual variance* (Barndorff-Nielsen & Shephard, 2002), then, we have the law of price transition as follows:

**Proposition 3.1.** *Given the values of asset price  $S_T$  and variance level  $V_T$  at time  $T \geq 0$ , the asset price at time  $T + \tau$  as the solution to the SDE (2.1, 2.2) is given by*

$$S_{T+\tau} = S_T \times e^\epsilon \times \prod_{i=1}^{\Delta N_\tau} e^{J_i} \times \prod_{j=1}^{\Delta N_\tau^*} e^{J_j^*} \times \exp\left(-\int_T^{T+\tau} c_s ds\right), \quad \tau \in \mathbb{R}^+, \quad (3.3)$$

or, in the logarithm of price as

$$\ln S_{T+\tau} = \ln S_T + \epsilon + \sum_{i=1}^{\Delta N_\tau} J_i + \sum_{j=1}^{\Delta N_\tau^*} J_j^* - (C_{T+\tau} - C_T), \quad (3.4)$$

where

$$\epsilon := r\tau - \frac{1}{2} \int_T^{T+\tau} V_s ds + \int_T^{T+\tau} \sqrt{V_s} dW_s,$$

and

$$\epsilon | I_{T+\tau} - I_T \sim \mathbf{N}\left(r\tau - \frac{1}{2}(I_{T+\tau} - I_T), I_{T+\tau} - I_T\right). \quad (3.5)$$

We know from Proposition 3.1 that, to simulate the price process  $S_{T+\tau}$  conditional on  $S_T$ , one has to first simulate the joint pair of shot-noise volatility and its integral together at time  $T + \tau$ , i.e.

$$(I_{T+\tau} - I_T, V_{T+\tau}) \mid I_T, V_T, S_T,$$

which relies on Theorem 3.1 derived as below.

**Theorem 3.1** (Joint Distribution of Shot-noise Volatility and Its Integral). *The joint Laplace transform of  $(Z_{T+\tau}, V_{T+\tau})$  conditional on  $(Z_T, V_T)$  is given by*

$$\mathbb{E}[e^{-\zeta Z_{T+\tau}} e^{-\xi V_{T+\tau}} | V_T, Z_T] = e^{-\zeta Z_T} e^{-\xi w V_T} \times \exp\left(-\varrho \int_T^{T+\tau} [1 - \hat{h}(\zeta + \xi e^{-\delta(T+\tau-s)})] ds\right), \quad \tau \in \mathbb{R}^+, \quad (3.6)$$

where  $w := e^{-\delta\tau}$  and

$$Z_t := \delta I_t + V_t. \quad (3.7)$$

Theorem 3.1 is proved in Appendix A.

**Corollary 3.1.** *The Laplace transform and mean of  $V_{T+\tau}$  conditional on  $V_T$  are given respectively by*

$$\mathbb{E}[e^{-\xi V_{T+\tau}} | V_T] = e^{-\xi w V_T} \times \exp\left(-\varrho \int_T^{T+\tau} [1 - \hat{h}(\xi e^{-\delta(T+\tau-s)})] ds\right), \quad \mathbb{E}[V_{T+\tau} | V_T] = V_0 e^{-\delta\tau} + \frac{\varrho}{\delta} \mu_H (1 - e^{-\delta\tau}). \quad (3.8)$$

The Laplace transform of asymptotic and stationary marginal distribution of  $V_{T+\tau}$  is

$$\hat{\Pi}(\xi) := \lim_{\tau \rightarrow \infty} \mathbb{E}[e^{-\xi V_{T+\tau}} | V_T] = \exp\left(-\frac{\varrho}{\delta} \int_0^\xi \frac{1 - \hat{h}(u)}{u} du\right). \quad (3.9)$$

**Proof.** Setting  $\zeta = 0$  in (3.6), we have the marginal distributions. Setting  $\zeta = 0$  and  $\tau = \infty$  in (3.6) and using the change of variable later as (3.10), the Laplace transform of the stationary marginal distribution of  $V_{T+\tau}$  is derived in (3.9).  $\square$

(3.8) offers a simple theoretical value later for validating and testing our simulation algorithms.

### 3.2. Simulation algorithms

Distributional properties derived in Section 3.1 reveal an elegant scheme for exact simulation. Let us first explain how to exactly sample a pair of increments of the numbers of two types of cojumps,  $(\Delta N_\tau, \Delta N_\tau^*)$ , the next intensity level  $\lambda_{T+\tau}$  and integrated intensity  $\Lambda_{T+\tau}$  conditional on the initial intensity level  $\lambda_T$  and the initial integrated intensity  $\Lambda_T$ , respectively, within the time period  $[T, T + \tau]$ :

**Algorithm 3.1** (Exact Simulation for  $\Delta N_\tau, \Delta N_\tau^*, \lambda_{T+\tau}, \Lambda_{T+\tau}$ ). *Conditional on the intensity level  $\lambda_T$  and integrated intensity  $\Lambda_T$ , reset  $T_0^* = T$ ,  $\lambda_{T_0^*} = \lambda_T$ ,  $n = n^* = 0$ , and execute the loop for  $k = 0, 1, 2, \dots$ :*

1. Simulate one candidate interarrival time  $E_{k+1}^*$  via

$$E_{k+1}^* = -\frac{1}{\varrho} \ln U, \quad U \sim \mathbf{U}[0, 1].$$

2. Simulate another candidate interarrival time  $S_{k+1}^*$  via

$$S_{k+1}^* = \begin{cases} S_{k+1}^{*(1)} \wedge S_{k+1}^{*(2)}, & \text{if } D_{k+1}^* > 0, \\ S_{k+1}^{*(2)}, & \text{if } D_{k+1}^* < 0, \end{cases}$$

where

$$D_{k+1}^* := 1 + \frac{\kappa \ln U_1}{\lambda_{T_k^*} - \mu_\lambda}, \quad U_1 \sim \mathbf{U}[0, 1],$$

and

$$S_{k+1}^{*(1)} := -\frac{1}{\kappa} \ln D_{k+1}^*; \quad S_{k+1}^{*(2)} := -\frac{1}{\mu_\lambda} \ln U_2, \quad U_2 \sim \mathbf{U}[0, 1].$$

3. Record the  $(k + 1)^{\text{th}}$  realised interarrival time  $\tau_{k+1}^*$  by

$$\tau_{k+1}^* = S_{k+1}^* \wedge E_{k+1}^*;$$

and then, record the  $(k + 1)^{\text{th}}$  jump-arrival time  $T_{k+1}^*$  in the intensity process  $\lambda_t$  by

$$T_{k+1}^* = T_k^* + \tau_{k+1}^*.$$

If  $T_{k+1}^* > T + \tau$ , then, terminate the entire loop, and output  $\Delta N_\tau, \Delta N_\tau^*, \lambda_{T+\tau}, \Lambda_{T+\tau}$  at the terminal time point  $T + \tau$  as

$$\begin{aligned} \Delta N_\tau &= n, \\ \Delta N_\tau^* &= n^*, \\ \lambda_{T+\tau} &= (\lambda_{T_k^*} - \mu_\lambda) e^{-\kappa(T+\tau-T_k^*)} + \mu_\lambda, \\ \Lambda_{T+\tau} &= \Lambda_{T_k^*} + \frac{\lambda_{T_k^*} - \mu_\lambda}{\kappa} [1 - e^{-\kappa(T+\tau-T_k^*)}] \\ &\quad + \mu_\lambda (T + \tau - T_k^*); \end{aligned}$$

otherwise, continue the following steps:

- Record the change at the jump-arrival time  $T_{k+1}^*$  in the process  $\lambda_t$  via

$$\lambda_{T_{k+1}^*} = \begin{cases} \lambda_{T_{k+1}^*} + Y_{k+1}^*, & \text{if } \tau_{k+1}^* = S_{k+1}^*, \\ \lambda_{T_{k+1}^*} - Y_{k+1}, & \text{if } \tau_{k+1}^* = E_{k+1}^*, \end{cases}$$

where

$$\lambda_{T_{k+1}^*} = (\lambda_{T_k^*} - \mu_\lambda) e^{-\kappa(T_{k+1}^* - T_k^*)} + \mu_\lambda.$$

- Record the increment in the integrated intensity process  $\Lambda_t$  within the period  $[T_k^*, T_{k+1}^*]$  via

$$\Lambda_{T_{k+1}^*} = \Lambda_{T_k^*} + \frac{\lambda_{T_k^*} - \mu_\lambda}{\kappa} (1 - e^{-\kappa \tau_{k+1}^*}) + \mu_\lambda \tau_{k+1}^*;$$

- Count the point increments of two types respectively via

$$\begin{aligned} n &= \begin{cases} n, & \text{if } \tau_{k+1}^* = S_{k+1}^*, \\ n + 1, & \text{if } \tau_{k+1}^* = E_{k+1}^*, \end{cases} \\ n^* &= \begin{cases} n^* + 1, & \text{if } \tau_{k+1}^* = S_{k+1}^*, \\ n^*, & \text{if } \tau_{k+1}^* = E_{k+1}^*. \end{cases} \end{aligned}$$

Algorithm 3.1 can be considered as an extension of the exact simulation scheme developed by Dassios and Zhao (2013) for the popular Hawkes process (Hawkes, 1971). It serves as an intermediate step for our main result Algorithm 3.2 for exactly simulating the shot-noise cojump framework as below.

**Algorithm 3.2** (Exact Simulation of Shot-noise Cojumps). Conditional on the initial values  $(S_T, V_T, I_T, \lambda_T, \Lambda_T)$  at time  $T$ ,  $(S_{T+\tau}, V_{T+\tau}, I_{T+\tau}, \lambda_{T+\tau}, \Lambda_{T+\tau})$  at time  $T + \tau$  for any  $\tau \in \mathbb{R}^+$  can be exactly simulated jointly via

$$\begin{aligned} V_{T+\tau} | V_T &\stackrel{\mathcal{D}}{=} wV_T + \sum_{i=1}^{\Delta N_\tau} X_i, \\ I_{T+\tau} | I_T, V_{T+\tau} &\stackrel{\mathcal{D}}{=} I_T + \frac{1}{\delta} \left( V_T - V_{T+\tau} + \sum_{i=1}^{\Delta N_\tau} Y_i^V \right), \\ \ln S_{T+\tau} | S_T, I_T, V_{T+\tau}, \lambda_T, \Lambda_T, \Lambda_{T+\tau} &\stackrel{\mathcal{D}}{=} \ln S_T + \epsilon + \sum_{i=1}^{\Delta N_\tau} J_i + \sum_{j=1}^{\Delta N_\tau^*} J_j^* - (C_{T+\tau} - C_T), \end{aligned}$$

where  $w := e^{-\delta\tau}$ ,

$$C_{T+\tau} - C_T = (\mu_S - 1)\varrho\tau + (\mu^* - 1)(\Lambda_{T+\tau} - \Lambda_T),$$

- $\Delta N_\tau$  is a Poisson random variable of rate  $\delta\tau$ , which can be exactly simulated all together with  $\Delta N_\tau^*, \lambda_{T+\tau}, \Lambda_{T+\tau}$  conditional on  $\lambda_T, \Lambda_T$  via Algorithm 3.1;

- $X_i$  and  $Y_i^V$  are dependent:

$$X_i | Y_i^V = y \stackrel{\mathcal{D}}{=} yw^{U_i}, \quad U_i \sim \mathbf{U}[0, 1];$$

- $\epsilon$  conditional on  $I_{T+\tau} - I_T$  is a normally distributed random variable, i.e.,

$$\epsilon | I_{T+\tau} - I_T \sim \mathbf{N}\left(r\tau - \frac{1}{2}(I_{T+\tau} - I_T), I_{T+\tau} - I_T\right).$$

**Proof.** The proof here focuses on the shot-noise SV part, which is integrated with the one for Algorithm 3.1. Since the jump size in volatility,  $Y_i^V$ , has the marginal density function  $dH(y)$ , we have

$$\begin{aligned} &\int_T^{T+\tau} [1 - \hat{h}(\zeta + \xi e^{-\delta(T+\tau-s)})] ds \\ &= \int_0^\tau [1 - \hat{h}(\zeta + \xi e^{-\delta x})] dx \\ &= \frac{1}{\delta} \int_{\zeta+\xi}^{\zeta+\xi e^{-\delta\tau}} \frac{1 - \hat{h}(u)}{\zeta - u} du \\ &= \frac{1}{\delta} \int_{u=\zeta+\xi}^{\zeta+\xi e^{-\delta\tau}} \frac{1}{\zeta - u} \int_{y=0}^\infty (1 - e^{-uy}) dH(y) du \\ &= -\frac{1}{\delta} \int_{v=\xi}^{\xi e^{-\delta\tau}} \frac{1}{v} \int_{y=0}^\infty [1 - e^{-(v+\zeta)y}] dH(y) dv \\ &= \frac{1}{\delta} \int_{y=0}^\infty \int_{z=0}^1 \frac{1}{z} [1 - e^{-(\xi z + \zeta)y}] dH(y) dz \\ &= \tau \int_{y=0}^\infty \int_{x=0}^\infty (1 - e^{-\xi x - \zeta y}) \frac{1}{\delta\tau x} \mathbf{1}_{[yw, y]} dx dH(y). \end{aligned} \tag{3.10}$$

Hence, by Theorem 3.1, the joint Laplace transform of  $(Z_{T+\tau}, V_{T+\tau})$  is

$$\begin{aligned} &\mathbb{E}[e^{-\zeta Z_{T+\tau}} e^{-\xi V_{T+\tau}} | V_T, Z_T] \\ &= e^{-\zeta Z_T} e^{-\xi w V_T} \\ &\quad \times \exp\left(-\varrho\tau \int_0^\infty \int_0^\infty (1 - e^{-\xi x - \zeta y}) \frac{1}{\delta\tau x} \mathbf{1}_{[yw, y]} h(y) dx dy\right) \\ &= e^{-\zeta Z_T} e^{-\xi w V_T} \times \exp(-\varrho\tau [1 - \hat{g}_{X, Y}(\zeta, \zeta)]), \end{aligned}$$

where the joint Laplace transform of the two random variables  $(X, Y)$  is

$$\begin{aligned}\hat{g}_{X,Y}(\xi, \zeta) &:= \mathbb{E}[e^{-\xi X} e^{-\zeta Y}] \\ &= \int_0^\infty \int_0^\infty e^{-\xi x - \zeta y} f_{X,Y}(x, y) dx dy,\end{aligned}$$

and the joint density function of  $(X, Y)$  is specified by

$$f_{X,Y}(x, y) = \frac{1}{\delta \tau x} \mathbf{1}_{[yw, y]} h(y), \quad (3.11)$$

which is well-defined since

$$\begin{aligned}\int_0^\infty \int_0^\infty f_{X,Y}(x, y) dx dy &= \int_0^\infty \int_0^\infty \frac{1}{\delta \tau x} \mathbf{1}_{[yw, y]} h(y) dx dy \\ &= \int_0^\infty \left[ \left( \frac{1}{\delta \tau} \ln x \right) \Big|_{x=yw}^{x=y} \right] h(y) dy \\ &= \int_0^\infty h(y) dy = 1.\end{aligned}$$

Note that, the marginal density function of  $Y$  is given by

$$\begin{aligned}f_Y(y) &= \int_0^\infty f_{X,Y}(x, y) dx = \int_0^\infty \frac{1}{\delta \tau x} \mathbf{1}_{[yw, y]} h(y) dx \\ &= h(y) \int_0^\infty \frac{1}{\delta \tau x} \mathbf{1}_{[yw, y]} dx = h(y),\end{aligned}$$

which implies  $Y \sim H$ . By conditioning, we have

$$f_{X,Y}(x, y) = f_Y(y) \times f_{X|Y=y}(x),$$

and  $X|Y=y$  has the conditional density of

$$f_{X|Y=y}(x) = \frac{1}{\delta \tau x} \mathbf{1}_{[yw, y]},$$

and can be simulated exactly via explicitly inverting the cumulative distribution function (CDF)

$$F_{X|Y=y}(x) = \frac{1}{\delta \tau} \ln \left( \frac{x}{yw} \right) \mathbf{1}_{[yw, y]},$$

with the analytic inverse

$$F_{X|Y=y}^{-1}(u) = ywe^{\delta \tau u}, \quad u \in [0, 1],$$

i.e.

$$\begin{aligned}X|Y=y &\stackrel{\mathcal{D}}{=} ywe^{\delta \tau U^*} = ye^{-\delta \tau(1-U^*)} \stackrel{\mathcal{D}}{=} ye^{-\delta \tau U^*} \\ &= yw^{U^*}, \quad U^* \sim \mathbf{U}[0, 1].\end{aligned}$$

It tells us how to exactly sample  $(Z_{T+\tau}, V_{T+\tau})$  conditional on  $(V_T, Z_T)$  pairwise and sequentially via

$$\begin{aligned}V_{T+\tau}|V_T &\stackrel{\mathcal{D}}{=} wV_T + \sum_{i=1}^{\Delta N_\tau} X_i, \\ Z_{T+\tau}|Z_T &\stackrel{\mathcal{D}}{=} Z_T + \sum_{i=1}^{\Delta N_\tau} Y_i^V,\end{aligned}$$

where  $X_i$  and  $Y_i$  are dependent following the joint PDF of (3.11). Based on the transform (3.7), we have  $I_{T+\tau} = \frac{1}{\delta}(Z_{T+\tau} - V_{T+\tau})$  and  $Z_T = \delta I_T + V_T$ . Together with Proposition 3.1 and Algorithm 3.1, we finally obtain Algorithm 3.2.  $\square$

### 3.3. Replicating marginal distributions of other SV models

This subsection is to demonstrate that, although this class of SV models is simple, its great flexibility of choosing jump-size distributions is able to mimic the marginal distributions of many more sophisticated SV models whose exact simulation algorithms without numerical inversion and A/R (perfect decomposition) are not available. For example, it can marginally match any marginal distribution of very popular non-Gaussian OU SV models introduced by Barndorff-Nielsen and Shephard (2001a, 2002) (BNS). Note that, this matching is not asymptotic, and in fact, it is exact in distribution.

**Proposition 3.2.** For any BNS' SV model with non-Gaussian OU SV process  $V_t^*$ ,

$$dV_t^* = -\delta V_t^* dt + dL_{\delta t}, \quad t \geq 0,$$

where  $L_t$  is a Lévy subordinator with Lévy measure  $\nu^*$ , if the CDF of volatility-jump sizes  $Y_t^V$  in the shot-noise SV process  $V_t$  is set by

$$H(y) = 1 - \frac{\delta}{q} y \frac{\nu^*(dy)}{dy}, \quad y \in \mathcal{Y}, \quad (3.12)$$

where the support  $\mathcal{Y} \subseteq [0, \infty)$  is determined by the specification of  $\nu^*$  such that  $H(y)$  is a well defined CDF, then, the marginal distributions of  $V_t$  and  $V_t^*$  are identical.

The proof is provided in Appendix B. For illustration, we provide two popular specifications of Lévy measure  $\nu^*$  for BNS' SV models:

- If one wants to match to the BNS' SV with gamma marginal distribution with shape parameter  $a^*$  and rate parameter  $b^*$ , i.e.,

$$\nu^*(dy) = a^* y^{-1} e^{-b^* y} dy, \quad y > 0, \quad a^*, b^* > 0, \quad (3.13)$$

then, we have



$$H(y) = \begin{cases} 1 - \frac{\delta a^*}{\varrho} e^{-b^* y}, & y \in [y^+, \infty), \\ 0, & y \in [0, y^+), \end{cases} \quad y^+ := \frac{1}{b^*} \ln \left( \frac{\varrho}{\delta a^*} \right).$$

In particular, if  $a^* = \frac{\varrho}{\delta}$  and  $b^* = \alpha > 0$ , then, nicely we have  $y^+ = 0$  and

$$H(y) = 1 - e^{-\alpha y}, \quad y \geq 0,$$

which implies an exponential distribution of rate  $\alpha$  for jump sizes  $Y_t^V$  and exactly recovers the popular gamma-OU SV model (Roberts et al., 2004).

- If one wants to match to the BNS' SV with a positive exponentially tilted stable (ETS) marginal distribution, i.e.,

$$\nu^*(dy) = \frac{\theta^*}{y^{\alpha^*+1}} e^{-\beta^* y} dy, \quad y \geq 0, \quad \alpha^* \in (0, 1), \quad \beta^*, \theta^* \in \mathbb{R}^+, \tag{3.14}$$

then, we have

$$H(y) = \begin{cases} 1 - \frac{\delta \theta^*}{\varrho} \frac{e^{-\beta^* y}}{y^{\alpha^*}}, & y \in [y^+, \infty), \\ 0, & y \in [0, y^+), \end{cases}$$

where  $y^+$  is the unique positive solution to the equation of  $y$ ,

$$\frac{\delta \theta^*}{\varrho} \frac{e^{-\beta^* y}}{y^{\alpha^*}} = 1.$$

#### 4. Pricing options with shot-noise cojumps

In this section, we illustrate the performance, effectiveness and flexibility of our algorithms through extensive numerical experiments. Section 4.1 and 4.2 were implemented on a desktop with Intel Core i7-6700 CPU@3.40 GHz processor, 24.00GB RAM, Windows 10 Professional, 64-bit Operating System. Section 4.4 was implemented on a desktop with Intel Core i7-1165G7 CPU@3.40 GHz processor, 16.00GB RAM, Windows 10 Home, 64-bit Operating System. The algorithms are coded and performed in MatLab (R2012a), and the computing time is measured by the elapsed CPU time in seconds. Numerical validation and tests for our algorithms are based on the true values of expected volatility levels and asset prices in (3.8) and (3.2). The associated errors from the true values are reported by three standard measures:

1. Error (*Error*) = estimated value (*Est*) - true value;
2. Relative error (*Error %*) =  $\frac{\text{estimated value} - \text{true value}}{\text{true value}}$ ;
3. Root mean square error  $RMSE = \sqrt{\text{bias}^2 + SE^2}$ , where the *SE* is the standard error of the simulation output, and the bias is the difference between the expectation of the estimator and

the associated true (theoretical) value; for the algorithm of exact simulation here, the bias is set to zero.

As an example, we implement a simple application of our new scheme for pricing exotic options in finance. It is well known that, pricing exotic options under SV models is tricky. Discretely-monitored path-dependent options (such as discrete-barrier European, Asia, lookback options) usually have no closed forms for their prices (except for a very small number of monitoring instants under the simple Black-Scholes setting), and practitioners in the financial industry commonly use Monte Carlo simulation for evaluation (Campbell et al., 1997, p.340).<sup>6</sup> It is straightforward to directly apply our exact scheme, as only the prices at these monitoring time points need to be simulated, and the option prices thereby can be evaluated without bias. Here, we take the discretely-monitored barrier option as an example, which is one of the most commonly traded exotic options and is especially popular in foreign exchange markets. Although some analytical approximation approaches do exist, pricing path-dependent options using Monte Carlo simulation for advanced models is still widely adopted.

As a prototypical barrier option, let us consider a *down-and-out barrier option* on a European call or put with discrete monitoring instants  $\{t_k\}_{k=1,2,\dots,m-1}$  where  $t_k := k\Delta t$ ,  $\Delta = T/m$  and  $T > 0$  is the maturity (which is not the monitoring time point). For simplification, we denote  $S_k := S_{t_k}$ . The payoff function at time  $T$  is  $F_o(S_T)$  if  $S_k > b$  for all  $k = 1, 2, \dots, m-1$ , where  $F_o(s) = (S_T - K)^+$  for the call type,  $F_o(s) = (K - S_T)^+$  for the put type,  $b > 0$  is the fixed lower barrier, and  $K > b$  is the strike price. The present value of this option (at time  $t = 0$ ) is

$$\begin{aligned} & e^{-rT} \mathbb{E} \left[ \mathbf{1}_{\{\underline{M}_{[0,T]} > b\}} F_o(S_T) | S_0 \right] \\ &= e^{-rT} \mathbb{E} \left[ \prod_{k=1}^{m-1} \mathbf{1}_{\{S_k > b\}} F_o(S_T) | S_0 \right], \end{aligned}$$

where  $\mathbf{1}_{\{\cdot\}}$  is the indicator function, and

$$\underline{M}_{[0,T]} := \min_{1 \leq k \leq m-1} S_k.$$

Since  $\{S_k\}_{k=1,2,\dots,m}$  can be sequentially and exactly simulated via Algorithm 3.2 without time discretisation or numerical inversion, the option price at time  $t = 0$  can be estimated without bias. In fact, Algorithm 3.2 offers us a great flexibility to select various choices of distributions for cojump sizes, to investigate the associated impacts to the option prices. In the following two subsections, we offer two typical examples respectively to illustrate how Algorithm 3.2 can be implemented in details:

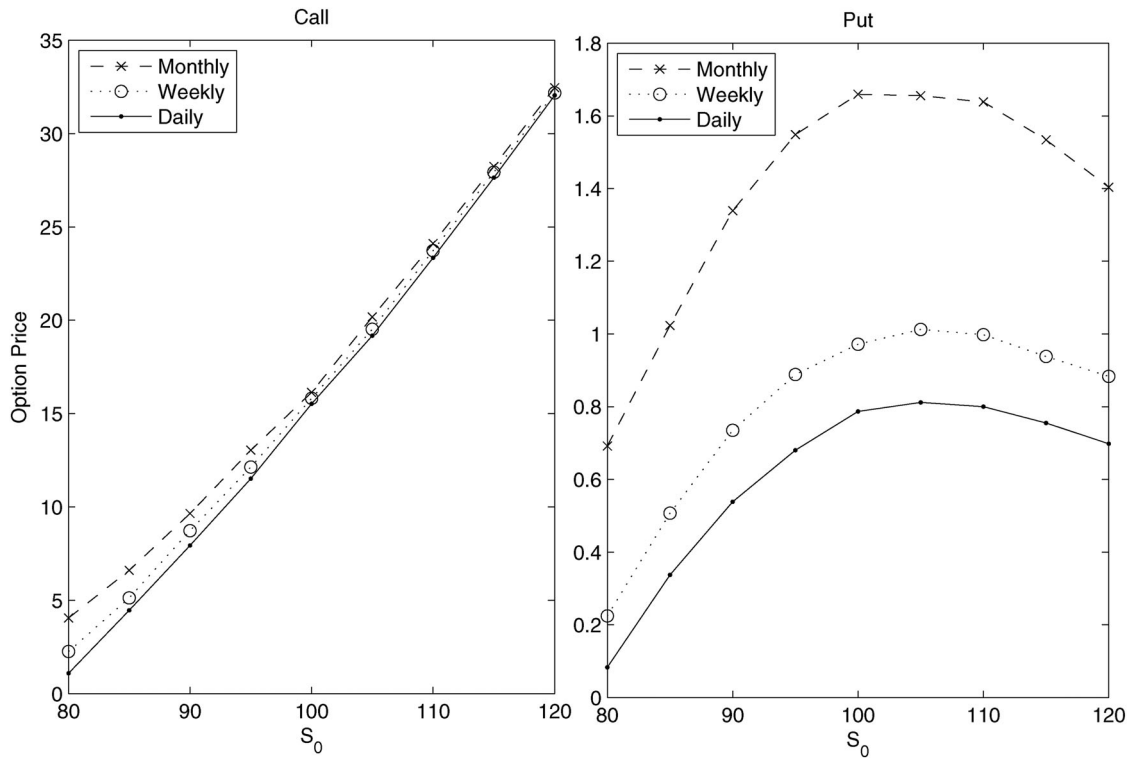


**Figure 2.** Unbiasedly estimated prices of monthly, weekly and daily monitored barriers on European call and put options respectively for  $S_0 \in [80, 120]$ , and each value point is estimated from 100, 000 sample paths, with the detailed numerical results reported in Table 1.

**Table 1.** Numerical results for the unbiasedly estimated prices of monthly, weekly and daily monitored barrier options respectively for  $S_0 \in [80, 120]$ , and each value point is estimated from 100, 000 sample paths, with the associated plots provided in Figure 2.

$S_0$	Call					Put									
	Call	RMSE	Put	RMSE	Time	Call	RMSE	Put	RMSE	Time					
	<b>Monthly</b>					<b>Weekly</b>					<b>Daily</b>				
80	4.05	0.06	0.69	0.010	45	2.26	0.05	0.22	0.005	172	1.08	0.03	0.08	0.003	801
85	6.60	0.07	1.02	0.012	44	5.13	0.06	0.51	0.008	171	4.46	0.06	0.34	0.006	792
90	9.65	0.08	1.34	0.014	43	8.73	0.08	0.74	0.009	174	7.93	0.08	0.54	0.008	813
95	13.04	0.10	1.55	0.015	44	12.13	0.09	0.89	0.010	171	11.52	0.09	0.68	0.008	789
100	16.14	0.10	1.66	0.016	44	15.82	0.10	0.97	0.011	170	15.53	0.11	0.79	0.009	795
105	20.17	0.12	1.66	0.016	44	19.52	0.12	1.01	0.011	169	19.17	0.12	0.81	0.009	793
110	24.11	0.13	1.64	0.016	45	23.73	0.13	1.00	0.011	168	23.34	0.13	0.80	0.009	777
115	28.24	0.14	1.53	0.015	44	27.94	0.14	0.94	0.010	170	27.64	0.14	0.76	0.009	775
120	32.46	0.15	1.40	0.015	45	32.18	0.15	0.88	0.010	168	32.05	0.15	0.70	0.008	786

1. The first example is simple and concise which is a pure shot-noise SV model without price-intensity cojumps (no contagion);
2. The second example is more realistic and comprehensive where there are fully two types of cojumps.

**4.1. Pure shot-noise SV models**

Let us first implement some simpler special cases of Definition 2.1, the shot-noise SV models without cojumps. Representatively, we adopt the popular choice of a positive exponentially tilted stable (ETS) distribution<sup>7</sup> as an example for demonstration, i.e.  $Y_i^V \sim \text{ETS}(\alpha, \beta, \theta)$  with its Lévy measure

$$\nu(dy) = \frac{\theta}{y^{\alpha+1}} e^{-\beta y} dy, \quad y \geq 0, \quad \alpha \in (0, 1),$$

$$\beta, \theta \in \mathbb{R}^+,$$

and mean  $\mu_H = \theta\beta^{\alpha-1}\Gamma(1 - \alpha)$ , where  $\alpha$  is the stability index,  $\theta$  is the intensity parameter and  $\beta$  is the tilting parameter. In practice, parameters should be calibrated from the prices of liquidly traded European options (i.e.  $m = 1$ ) when the data is available. Here, for the illustration purpose, the option contracts and parameters are manually set as

$$r = 5\%, \quad S_0 = 100, \quad K = 100, \quad T = 1, \quad b = 80,$$

$$V_0 = 0.2, \quad \mu_V = 0, \quad \varrho = 4, \quad \delta = 5,$$

$$\alpha = 0.25, \quad \beta = 1.5, \quad \theta = 0.2.$$

We adopt a highly efficient new algorithm in Dassios et al. (2018) for exactly sampling ETS random variables. The plots of unbiasedly estimated prices for the monthly ( $m = 12$ ), weekly ( $m = 52$ ) and daily ( $m = 250$ ) monitored barriers of European call and put options respectively for  $S_0 \in [80, 120]$

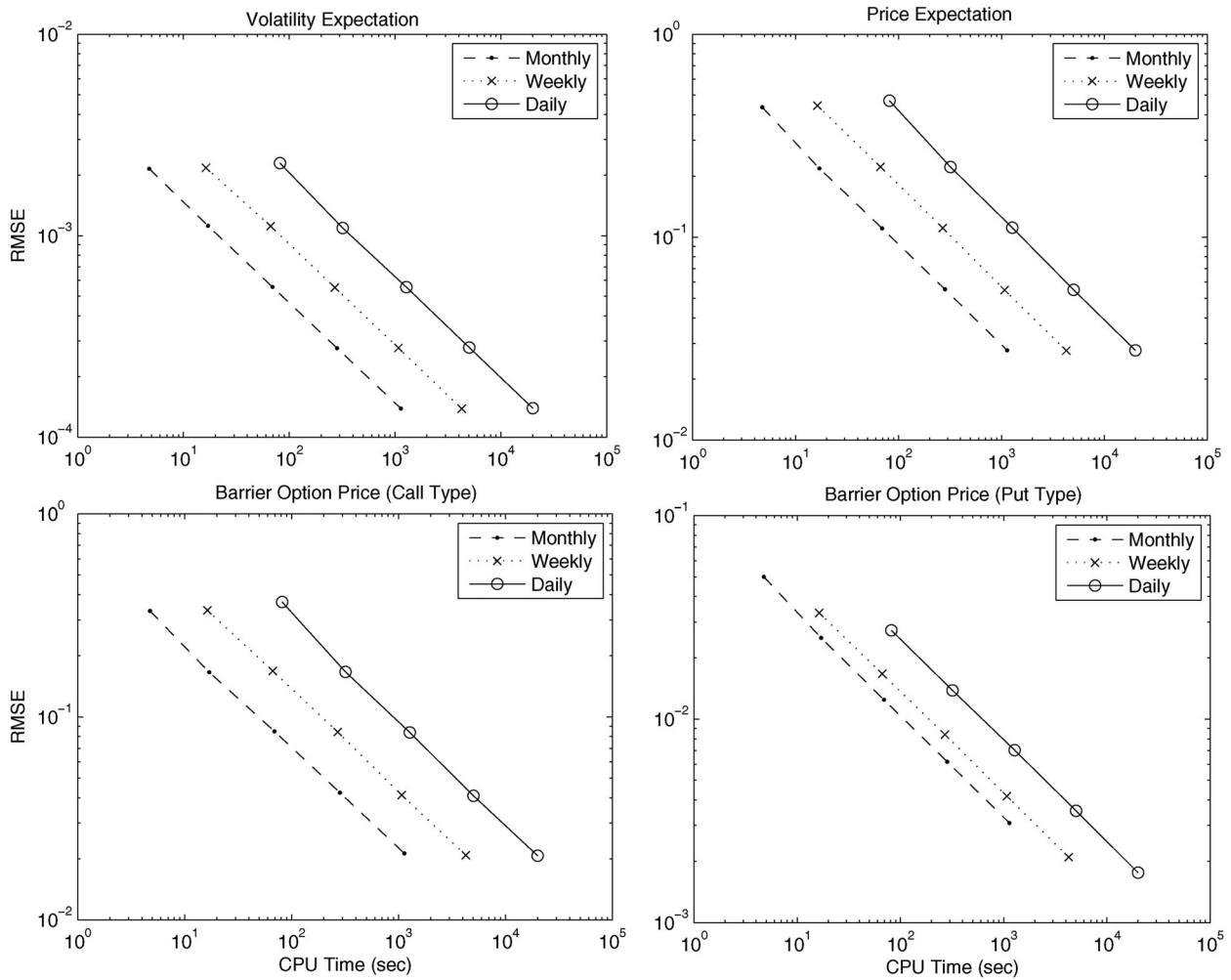


**Figure 3.** Convergence analysis of our exact simulation scheme (Algorithm 3.2) for unbiasedly estimated volatility expectation  $\mathbb{E}[V_T|V_0]$ , price expectation  $\mathbb{E}[S_T|S_0]$ , and option prices of monthly, weekly and daily monitored barriers on European call and put options respectively, with the associated numerical results reported in Table 2.

are presented in Figure 2. Each value point is estimated from 100, 000 sample paths, which are exactly simulated by Algorithm 3.2. The detailed numerical results are reported in Table 1. Thanks to the simple analytic formulas for true values of expected volatility level  $\mathbb{E}[V_T|V_0]$  and expected price level  $\mathbb{E}[S_T|S_0]$  available in (3.8) and (3.2), respectively, we are able to easily test the accuracy and efficiency of our algorithm. Convergence analysis of our exact simulation scheme (Algorithm 3.2) for unbiasedly estimated volatility expectation  $\mathbb{E}[V_T|V_0]$ , price expectation  $\mathbb{E}[S_T|S_0]$ , and option prices of monthly, weekly and daily monitored barriers on European call and put options are plotted in Figure 3, respectively, with the associated numerical results based in Table 2. In particular, we can observe that, the price of discretely monitored barriers on European put options is not monotone with respect to the initial stock price  $S_0$ , which is consistent with the finding in literature, see Feng and Linetsky (2008).

**4.2. Shot-noise cojump models with independent cojump sizes**

Now, let us carry out numerical experiments with more comprehensive settings where both two types of cojumps exist as fully specified by Definition 2.1. Let us first assume that cojump sizes in price, volatility and intensity are independent of each other as (Broadie et al., 2007, p.1457), and

$$Y_i^V \sim \text{Exp}(\alpha), \quad Y_i \sim \text{Exp}(\beta_1), \quad Y_j^* \sim \text{Exp}(\beta_2),$$

$$J_i \sim \text{N}(\mu_1, \sigma_1^2), \quad J_j^* \sim \text{N}(\mu_2, \sigma_2^2),$$

so, we have means

$$\mu_H = \frac{1}{\alpha}, \quad \mu_S = \mathbb{E}[e^{J_i}] = \exp\left(\mu_1 + \frac{1}{2}\sigma_1^2\right),$$

$$\mu^* = \mathbb{E}[e^{J_j^*}] = \exp\left(\mu_2 + \frac{1}{2}\sigma_2^2\right).$$

The parameters are set by

$$r = 5\%, S_0 = 100, K = 100, T = 1, b = 80, \quad (4.1)$$

**Table 2.** Numerical results for the convergence analysis of our exact simulation scheme (Algorithm 3.2) for unbiasedly estimated volatility expectation  $\mathbb{E}[V_T|V_0]$ , price expectation  $\mathbb{E}[S_T|S_0]$ , and option prices of monthly, weekly and daily monitored barriers on European call and put options respectively, with the associated plots provided in Figure 3.

Paths	$\mathbb{E}[V_T V_0]$					$\mathbb{E}[S_T S_0]$					Call		Put		Time
	True	Est	Error	Error%	RMSE	True	Est	Error	Error%	RMSE	Est	RMSE	Est	RMSE	
<b>Monthly</b>															
10,000	0.1450	0.1475	0.0025	1.73%	0.0021	105.1271	104.8687	-0.2584	-0.25%	0.4360	16.3582	0.3324	1.6409	0.0500	5
40,000	0.1450	0.1444	-0.0007	-0.46%	0.0011	105.1271	104.9893	-0.1378	-0.13%	0.2180	16.2253	0.1660	1.6709	0.0251	17
160,000	0.1450	0.1455	0.0005	0.34%	0.0006	105.1271	105.0092	-0.1179	-0.11%	0.1105	16.4153	0.0849	1.6605	0.0124	69
640,000	0.1450	0.1450	-0.0001	-0.05%	0.0003	105.1271	105.0876	-0.0395	-0.04%	0.0553	16.4446	0.0424	1.6409	0.0062	283
2,560,000	0.1450	0.1451	0.0000	0.03%	0.0001	105.1271	105.1603	0.0332	0.03%	0.0277	16.4988	0.0213	1.6421	0.0031	1,137
<b>Weekly</b>															
10,000	0.1450	0.1441	-0.0010	-0.66%	0.0022	105.1271	105.3827	0.2556	0.24%	0.4438	16.0692	0.3347	0.9625	0.0332	16
40,000	0.1450	0.1451	0.0000	0.02%	0.0011	105.1271	105.1002	-0.0269	-0.03%	0.2220	15.8009	0.1684	0.9845	0.0167	67
160,000	0.1450	0.1453	0.0002	0.17%	0.0006	105.1271	105.2642	0.1371	0.13%	0.1110	15.9575	0.0842	0.9858	0.0084	270
640,000	0.1450	0.1451	0.0000	0.02%	0.0003	105.1271	104.9996	-0.1275	-0.12%	0.0549	15.7039	0.0412	0.9853	0.0042	1,074
2,560,000	0.1450	0.1450	-0.0000	-0.01%	0.0001	105.1271	105.1184	-0.0088	-0.01%	0.0276	15.8166	0.0208	0.9875	0.0021	4,264
<b>Daily</b>															
10,000	0.1450	0.1484	0.0033	2.30%	0.0023	105.1271	105.0292	-0.0979	-0.09%	0.4705	15.4459	0.3681	0.7337	0.0273	82
40,000	0.1450	0.1439	-0.0011	-0.78%	0.0011	105.1271	105.1172	-0.0099	-0.01%	0.2214	15.3683	0.1666	0.7489	0.0138	320
160,000	0.1450	0.1453	0.0002	0.16%	0.0006	105.1271	105.2243	0.0972	0.09%	0.1113	15.3937	0.0838	0.7757	0.0070	1,277
640,000	0.1450	0.1451	0.0001	0.08%	0.0003	105.1271	105.0217	-0.1055	-0.10%	0.0551	15.2567	0.0409	0.7824	0.0035	5,031
2,560,000	0.1450	0.1451	0.0000	0.03%	0.0001	105.1271	105.1150	-0.0121	-0.01%	0.0277	15.3673	0.0207	0.7722	0.0018	20,032

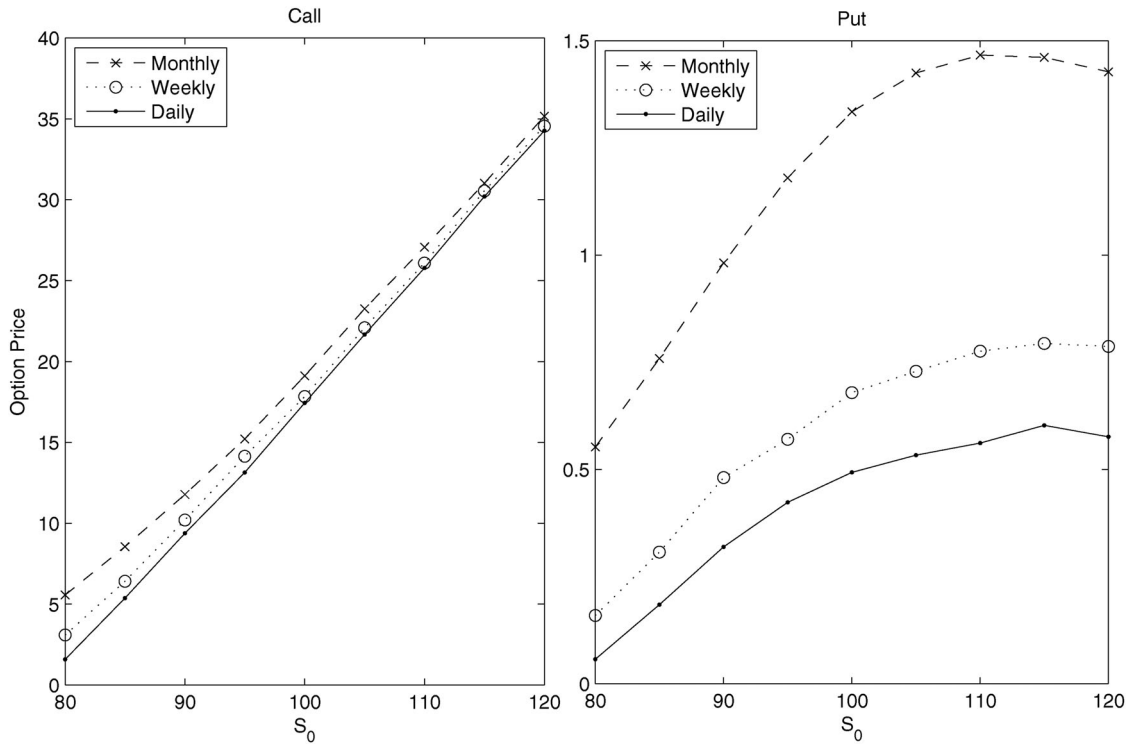


**Figure 4.** Unbiasedly estimated prices of monthly, weekly and daily monitored barriers on European call and put options respectively for  $S_0 \in [80, 120]$ , and each value point is estimated from 100, 000 sample paths, with the detailed numerical results reported in Table 3.

$$\begin{aligned}
 V_0 &= 0.25, & \mu_V &= 0, & \varrho &= 4, & \delta &= 5, & \alpha &= 5, \\
 \mu_1 &= \mu_2 &= 0, & \sigma_1 &= \sigma_2 &= 0.1,
 \end{aligned}
 \tag{4.2}$$

$$\lambda_0 = 0.5, \quad \mu_\lambda = 0.1, \quad \beta_1 = 2.5, \quad \beta_2 = 4. \tag{4.3}$$

Exactly sampled paths of the joint process  $(S_t, V_t, \lambda_t)$  are provided earlier in Figure 1. The plots of unbiasedly estimated prices for the monthly ( $m = 12$ ), weekly ( $m = 52$ ) and daily ( $m = 250$ ) moni-

tored barriers of European call and put options respectively for  $S_0 \in [80, 120]$  are presented in Figure 4, with detailed numerical results in Table 3. To test the accuracy and efficiency of our exact simulation scheme, convergence analysis for unbiasedly estimated volatility expectation  $\mathbb{E}[V_T|V_0]$ , price expectation  $\mathbb{E}[S_T|S_0]$ , and option prices of monthly, weekly and daily monitored barriers on European call and put options are plotted in Figure 5, respectively, with the associated numerical results reported in Table 4.

**Table 3.** Numerical results for the unbiasedly estimated prices of monthly, weekly and daily monitored barrier options respectively for  $S_0 \in [80, 120]$ , and each value point is estimated from 100, 000 sample paths, with the associated plots provided in Figure 4.

$S_0$	Call	RMSE	Put	RMSE	Time	Call	RMSE	Put	RMSE	Time	Call	RMSE	Put	RMSE	Time
	Monthly					Weekly					Daily				
80	5.56	0.0730	0.55	0.0099	47	3.10	0.0579	0.16	0.0046	161	1.58	0.0405	0.06	0.0026	784
85	8.55	0.0892	0.76	0.0115	46	6.41	0.0818	0.31	0.0064	161	5.37	0.0740	0.18	0.0046	784
90	11.78	0.1045	0.98	0.0131	46	10.20	0.0998	0.48	0.0079	162	9.38	0.0968	0.32	0.0060	782
95	15.22	0.1182	1.18	0.0142	45	14.14	0.1154	0.57	0.0085	162	13.14	0.1128	0.42	0.0068	777
100	19.11	0.1329	1.33	0.0152	46	17.83	0.1300	0.68	0.0093	161	17.44	0.1303	0.49	0.0074	776
105	23.26	0.1477	1.42	0.0157	46	22.08	0.1441	0.73	0.0096	162	21.67	0.1441	0.53	0.0077	769
110	27.07	0.1576	1.47	0.0159	46	26.08	0.1548	0.78	0.0099	162	25.78	0.1574	0.56	0.0078	785
115	31.02	0.1697	1.46	0.0158	46	30.55	0.1690	0.79	0.0100	162	30.20	0.1704	0.60	0.0081	768
120	35.17	0.1780	1.43	0.0155	47	34.55	0.1807	0.79	0.0100	163	34.26	0.1796	0.58	0.0079	754

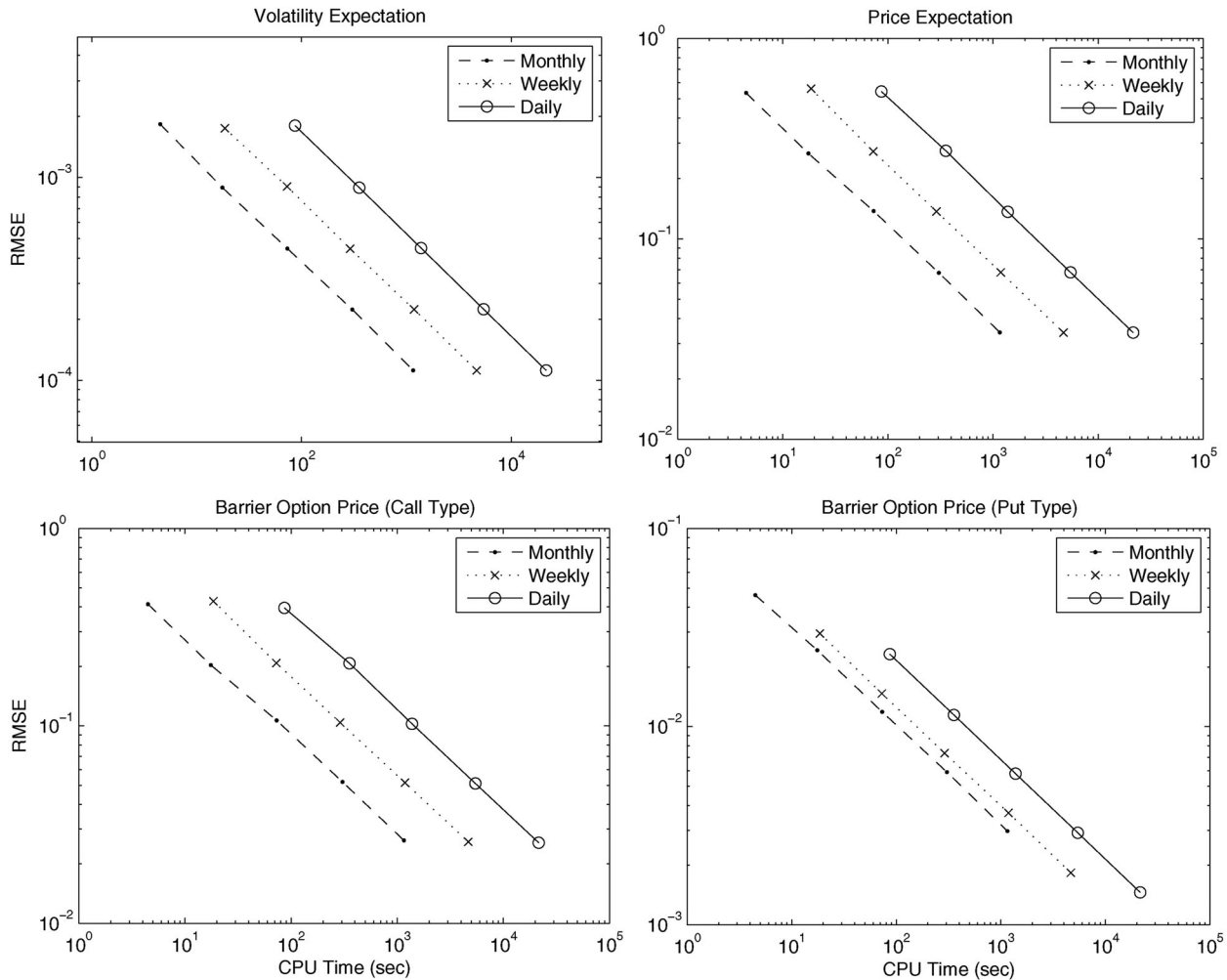


**Figure 5.** Convergence analysis of our exact simulation scheme (Algorithm 3.2) for unbiasedly estimated volatility expectation  $\mathbb{E}[V_T|V_0]$ , price expectation  $\mathbb{E}[S_T|S_0]$ , and option prices of monthly, weekly and daily monitored barriers on European call and put options respectively, with the associated numerical results reported in Table 4.

**4.3. Shot-noise cojump models with dependent cojump sizes**

Some empirical evidences show the occurrence of jumps in price and volatility changes is of opposite sign (Bandi & Renò, 2016) that further strengths” leverage effects”. More generally,  $Q(y_1, y_2, y_3)$ , the dependency of the sizes of price-volatility-intensity cojumps  $\{(J_i, Y_i^V, Y_i)\}_{i=1,2,\dots}$ , and  $Q^*(x_1, x_2)$ , the dependency of the sizes of price-intensity cojumps  $\{(J_j^*, Y_j^*)\}_{j=1,2,\dots}$ , can be constructed, for example,

via two copula functions, respectively<sup>8</sup>, e.g. one 3-dimensional Gaussian copula  $\mathbb{C}_1$  for  $Q(y_1, y_2, y_3)$  and one 2-dimensional Gaussian copula  $\mathbb{C}_2$  for  $Q^*(x_1, x_2)$ . More precisely, we can assume that,

$$Y_i^V \sim \text{Exp}(\alpha), \quad Y_i \sim \text{Exp}(\beta_1), \quad J_i \sim \mathcal{N}(\mu_1, \sigma_1^2),$$

and they can be simulated dependently via

$$Y_i^V \stackrel{\mathcal{D}}{=} -\frac{1}{\alpha} \ln U_i^{(1)}, \quad Y_i \stackrel{\mathcal{D}}{=} -\frac{1}{\beta_1} \ln U_i^{(2)},$$

$$J_i \stackrel{\mathcal{D}}{=} \mu_1 + \sigma_1 \Phi^{-1}(U_i^{(3)}),$$

**Table 4.** Numerical results for the convergence analysis of our exact simulation scheme (Algorithm 3.2) for unbiasedly estimated volatility expectation  $\mathbb{E}[V_T|V_0]$ , price expectation  $\mathbb{E}[S_T|S_0]$ , and option prices of monthly, weekly and daily monitored barriers on European call and put options respectively, with the associated plots provided in Figure 5.

Paths	$\mathbb{E}[V_T V_0]$					$\mathbb{E}[S_T S_0]$					Call		Put		Time
	True	Est	Error	Error%	RMSE	True	Est	Error	Error%	RMSE	Est	RMSE	Est	RMSE	
<b>Monthly</b>															
10,000	0.1606	0.1623	0.0017	1.06%	0.0018	105.1271	105.4142	0.2871	0.27%	0.5347	19.1815	0.4135	1.2390	0.0461	4
40,000	0.1606	0.1609	0.0003	0.20%	0.0009	105.1271	104.9003	-0.2268	-0.22%	0.2667	19.0091	0.2032	1.3422	0.0243	18
160,000	0.1606	0.1610	0.0004	0.22%	0.0004	105.1271	105.2863	0.1592	0.15%	0.1375	19.2416	0.1065	1.3121	0.0119	73
640,000	0.1606	0.1606	-0.0000	0.00%	0.0002	105.1271	104.9513	-0.1758	-0.17%	0.0677	19.0106	0.0520	1.3090	0.0059	305
2,560,000	0.1606	0.1606	0.0000	0.01%	0.0001	105.1271	105.0976	-0.0295	-0.03%	0.0341	19.0939	0.0263	1.3179	0.0030	1,159
<b>Weekly</b>															
10,000	0.1606	0.1590	-0.0016	-1.02%	0.0017	105.1271	105.0265	-0.1006	-0.10%	0.5612	18.3134	0.4281	0.6823	0.0295	19
40,000	0.1606	0.1616	0.0010	0.63%	0.0009	105.1271	105.4061	0.2789	0.27%	0.2731	18.1809	0.2081	0.6835	0.0147	73
160,000	0.1606	0.1605	-0.0001	-0.04%	0.0004	105.1271	105.2869	0.1598	0.15%	0.1369	18.1562	0.1039	0.6813	0.0074	290
640,000	0.1606	0.1605	-0.0001	-0.04%	0.0002	105.1271	104.9936	-0.1335	-0.13%	0.0680	17.9316	0.0516	0.6788	0.0037	1,184
2,560,000	0.1606	0.1605	-0.0001	-0.06%	0.0001	105.1271	105.1186	-0.0085	-0.01%	0.0340	18.0620	0.0258	0.6772	0.0018	4,672
<b>Daily</b>															
10,000	0.1606	0.1634	0.0028	1.73%	0.0018	105.1271	105.2241	0.0970	0.09%	0.5427	17.4242	0.3961	0.4786	0.0232	87
40,000	0.1606	0.1600	-0.0006	-0.35%	0.0009	105.1271	105.2702	0.1431	0.14%	0.2750	17.5493	0.2075	0.4782	0.0114	356
160,000	0.1606	0.1612	0.0006	0.38%	0.0004	105.1271	105.1283	0.0012	0.00%	0.1363	17.4453	0.1025	0.4891	0.0058	1,382
640,000	0.1606	0.1606	0.0000	0.00%	0.0002	105.1271	105.1090	-0.0181	-0.02%	0.0681	17.3836	0.0511	0.4920	0.0029	5,452
2,560,000	0.1606	0.1607	0.0001	0.06%	0.0001	105.1271	105.1080	-0.0191	-0.02%	0.0341	17.4070	0.0256	0.4923	0.0015	21,542

where  $(U_i^{(1)}, U_i^{(2)}, U_i^{(3)})$  is a vector of dependent uniform random variables from copula  $\mathcal{C}_1$ , and  $\Phi$  is the CDF of a standard normal distribution. Similarly, we assume

$$Y_j^* \sim \text{Exp}(\beta_2), \quad J_j^* \sim \text{N}(\mu_2, \sigma_2^2),$$

and they can be simulated dependently via

$$Y_j^* \stackrel{\mathcal{D}}{=} -\frac{1}{\beta_2} \ln U_j^{[1]}, \quad J_j^* \stackrel{\mathcal{D}}{=} \mu_2 + \sigma_2 \Phi^{-1}(U_j^{[2]}),$$

where  $(U_j^{[1]}, U_j^{[2]})$  is a vector of dependent uniform random variables from copula  $\mathcal{C}_2$ . As the associated results would present similar numerical structure as the precious cases, to avoid repetition here we just illustrate this main idea. Of course, instead we may use other copulas, such as student- $t$  copulas that can incorporate tail dependency.

**4.4. Comparison: Exact scheme v.s. Discretisation scheme**

The shot-noise cojump models introduced in this paper are new, and there is no existing simulation algorithm that can be used directly in the literature. The classical discretisation scheme can be developed to apply to our models, and we can provide a comparison between our exact scheme with discretisation scheme. Although discretisation scheme is widely used, particularly in the industry, it is well known that this scheme introduces bias into estimation and the associated bias is hard to be quantified and measured, see e.g. Glasserman (2003) and Asmussen and Glynn (2007) for more discussions.

The classical (Euler) discretisation scheme can be applied to approximate our shot-noise cojump framework by discretising the SDEs in Definition

2.1 with the equally-spaced small time interval (grid) of length  $\Delta > 0$  as

$$\frac{\hat{S}_{t+\Delta} - \hat{S}_t}{\hat{S}_t} = (r - c_t)\Delta + \sqrt{\hat{V}_t}(W_{t+\Delta} - W_t)$$

$$+ (e^{J_t} - 1)(N_{t+\Delta} - N_t)$$

$$+ (e^{J_t^*} - 1)(N_{t+\Delta}^* - N_t^*),$$

$$\hat{V}_{t+\Delta} - \hat{V}_t = -\delta(\hat{V}_t - \mu_V)\Delta + Y_t^V(N_{t+\Delta} - N_t),$$

$$\hat{\lambda}_{t+\Delta} - \hat{\lambda}_t = -\kappa(\hat{\lambda}_t - \mu_\lambda)\Delta + Y_t(N_{t+\Delta} - N_t)$$

$$+ Y_t^*(N_{t+\Delta}^* - N_t^*),$$

$$c_t = (\mu_S - 1)\varrho + (\mu^* - 1)\hat{\lambda}_t,$$

where  $(W_{t+\Delta} - W_t) \sim \text{N}(0, \Delta)$ ,  $(N_{t+\Delta} - N_t) \sim \text{Poisson}(\varrho\Delta)$  and  $(N_{t+\Delta}^* - N_t^*) \sim \text{Poisson}(\lambda_t\Delta)$ . Given the initial values  $(\hat{S}_0, \hat{V}_0, \hat{\lambda}_0) = (S_0, V_0, \lambda_0)$ , we can recursively simulate the discretised paths  $\{(\hat{S}_t, \hat{V}_t, \hat{\lambda}_t)\}_{t=1,2,\dots}$  for approximating the original processes  $\{(S_t, V_t, \lambda_t)\}_{t>0}$ . This discretisation is an approximation as it introduces bias, i.e. in theory  $\mathbb{E}[\hat{S}_t|\hat{S}_0] \neq \mathbb{E}[S_t|S_0]$  for any time point  $t > 0$ .

Based on the principle of optimal allocation of computation budget proposed by Duffie and Glynn (1995) for discretisation scheme, the number of time-discretisation grids is set equal to the square root of the number of sample paths. The numerical results of the comparison between the discretisation scheme and our exact scheme for estimated price expectation  $\mathbb{E}[S_T|S_0]$  based on the parameter setting in (4.1), (4.2) and (4.3) with  $T=1$  and  $T=10$ , respectively, are provided in Table 5. Our exact scheme is extremely fast, as Algorithm 3.2 applies to any time interval  $\tau \in \mathbb{R}^+$ . There is no need for multiple grids and one realisation of stock price level  $S_T$  can be directly simulated just by a single grid at the terminal time  $T$ . For example, 640,000 paths for  $T=10$  can be generated from our exact

scheme in only about 18.5s, whereas discretisation scheme takes about 10,287.7 seconds to achieve a similar level of accuracy. In addition, the graphic comparison of convergence via the RMSE versus CPU time is plotted in Figure 6. Although the discretisation scheme is easier for implementation, our exact scheme produces much smaller RMSE for a given computational budget. Hence, our exact scheme substantially outperforms the classical discretisation scheme.

**4.5. Performance sensitivity analysis**

Finally, the numerical analysis of performance sensitivity to the parameter choice is provided in Table 6 with the parameter setting in (4.1), (4.2) and (4.3) as the reference by varying one of parameters. As the sensitivity of algorithm performance to any of the

**Table 5.** Numerical results for the convergence analysis of our exact scheme (Algorithm 3.2) and discretisation scheme for estimated price expectation  $\mathbb{E}[S_T|S_0]$  for  $T=1, 10$ , respectively, with the associated plots provided in Figure 6.

Paths	Grids	True	Est	Error%	RMSE	Time (sec)
<b>Exact T = 1</b>						
10,000		105.1271	104.6699	-0.4349%	0.5475	0.3
40,000		105.1271	104.9415	-0.1765%	0.2748	0.9
160,000		105.1271	105.1566	0.0280%	0.1380	3.5
640,000		105.1271	105.1924	0.0621%	0.0684	4.6
<b>Discretisation T = 1</b>						
10,000	100	105.1271	104.3922	-0.6991%	0.9169	12.2
40,000	200	105.1271	105.3217	0.1851%	0.3377	118.5
160,000	400	105.1271	104.8970	-0.2189%	0.2670	1,258.8
640,000	800	105.1271	105.1069	-0.0193%	0.0711	9,261.8
<b>Exact T = 10</b>						
10,000		164.8721	169.4088	2.7516%	6.2396	0.9
40,000		164.8721	167.5343	1.6147%	3.2777	1.2
160,000		164.8721	165.3605	0.2962%	1.3237	3.6
640,000		164.8721	165.7269	0.5185%	0.6826	18.5
<b>Discretisation T = 10</b>						
10,000	100	164.8721	168.0074	1.9016%	6.8183	13.5
40,000	200	164.8721	164.3272	-0.3305%	2.7392	112.7
160,000	400	164.8721	162.5822	-1.3889%	2.7799	906.8
640,000	800	164.8721	164.4456	-0.2587%	0.8304	10,287.7

parameters of jump sizes is determined by the choice of distribution for jump sizes itself rather than our general exact scheme (Algorithm 3.2) which is distribution-free for jump sizes. It does not make much sense to analyse the sensitivity to these jump-size parameters. To analyse the sensitivity of our exact scheme, here, we focus on other parameters,  $S_0, \delta, \rho$  and  $\kappa$  as examples. We can observe that the parameter choice makes almost no impact to the computing time and the error measured by Error% of our proposed exact scheme (Algorithm 3.2), and the error measured by RMSE is also not very sensitive.

**5. Concluding remarks**

Shot-noise cojump framework, a class of shot-noise SV models with two types of cojumps, is appealing for financial applications on grounds of simplicity and tractability, and offers a parsimonious alternative for more sophisticated SV models in the literature. The great flexibility for jump-size distributions and its dependency among cojump sizes makes it able to replicate the marginal behaviours of many more sophisticated SV models, such as the classical non-Gaussian OU SV models. The associated algorithms for exact simulation developed are efficient, accurate, easy to use, and this is the main contribution of this paper. Neither numerical inversion nor A/R scheme is required, which means that it is not only accurate but also the efficiency would not be sensitive to the parameter choice, and this is the key methodological distinction from other existing exact algorithms for SV models. Our algorithm is extremely fast, and substantially outperforms the classical discretisation scheme. It might be also useful to fast generate sufficient amount of data for unbiasedly testing some newly developed statistical and econometrical methods for cojumps.

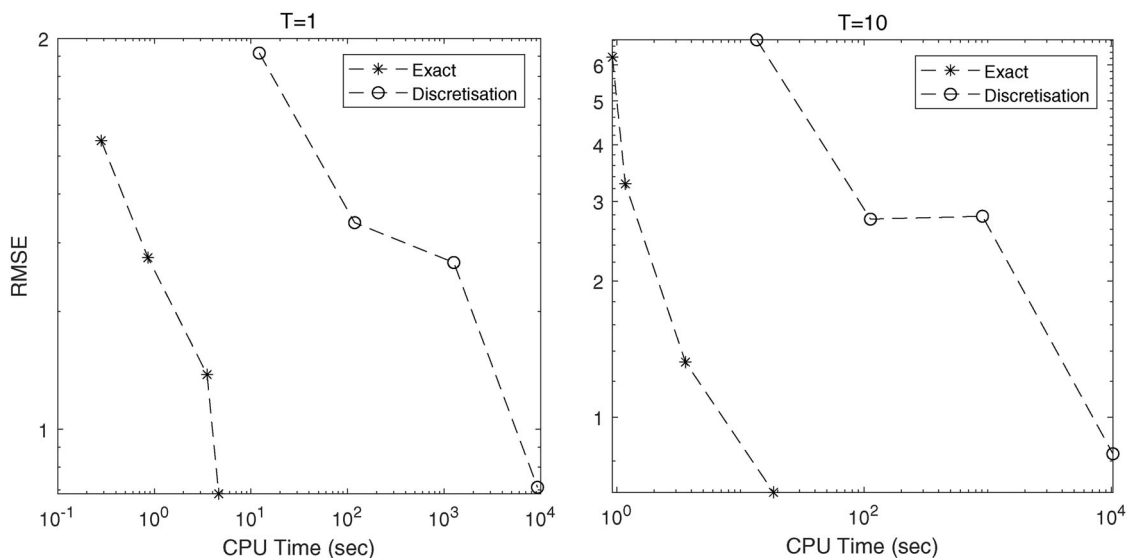


**Figure 6.** Convergence analysis of our exact scheme (Algorithm 3.2) and discretisation scheme for estimated price expectation  $\mathbb{E}[S_T|S_0]$  for  $T=1, 10$ , respectively, with the associated numerical results reported in Table 5.

**Table 6.** Sensitivity analysis of parameter settings for our exact scheme (Algorithm 3.2) for estimated price expectation  $\mathbb{E}[S_T|S_0]$  when  $T=1$  based on 640,000 sample paths.

$S_0$	True	Est	Error%	RMSE	Time (sec)
100	105.1271	105.1924	0.0621%	0.0684	4.6
110	115.6398	115.6583	0.0160%	0.0749	4.8
120	126.1525	126.2217	0.0548%	0.0822	5.2
130	136.6652	136.6384	-0.0196%	0.0884	4.9
140	147.1780	147.0044	-0.1179%	0.0950	4.6
150	157.6907	157.5816	-0.0692%	0.1023	4.8
160	168.2034	168.2636	0.0358%	0.1092	4.8
170	178.7161	178.6336	-0.0461%	0.1160	4.7
180	189.2288	189.0715	-0.0831%	0.1223	5.4
190	199.7415	199.5096	-0.1161%	0.1294	4.9
200	210.2542	210.1734	-0.0385%	0.1364	4.8
$\delta$	True	Est	Error%	RMSE	Time (sec)
1	105.1271	104.9545	-0.1642%	0.1110	4.9
2	105.1271	105.0416	-0.0814%	0.0940	4.8
3	105.1271	105.1766	0.0471%	0.0825	4.7
4	105.1271	105.0722	-0.0523%	0.0739	5.2
5	105.1271	105.1217	-0.0052%	0.0682	4.8
6	105.1271	105.0992	-0.0265%	0.0637	4.6
7	105.1271	105.0857	-0.0394%	0.0601	4.8
8	105.1271	105.1569	0.0284%	0.0577	4.6
9	105.1271	105.1612	0.0324%	0.0554	4.9
10	105.1271	105.2080	0.0770%	0.0537	4.8
$\bar{\sigma}$	True	Est	Error%	RMSE	Time (sec)
1	105.1271	105.1914	0.0611%	0.0427	5.1
2	105.1271	105.0292	-0.0932%	0.0522	4.9
3	105.1271	105.0340	-0.0885%	0.0604	4.9
4	105.1271	105.2329	0.1006%	0.0684	4.6
5	105.1271	105.0969	-0.0287%	0.0752	5.1
6	105.1271	105.2078	0.0767%	0.0824	4.9
7	105.1271	105.0934	-0.0321%	0.0884	4.8
8	105.1271	105.0625	-0.0615%	0.0955	4.9
9	105.1271	105.0238	-0.0983%	0.1024	4.6
10	105.1271	105.2205	0.0888%	0.1079	5.4
$\kappa$	True	Est	Error%	RMSE	Time (sec)
0.1	105.1271	105.1859	0.0559%	0.0685	4.7
0.2	105.1271	105.1912	0.0609%	0.0686	4.6
0.3	105.1271	105.1569	0.0284%	0.0684	4.5
0.4	105.1271	105.0307	-0.0917%	0.0681	4.7
0.5	105.1271	105.1158	-0.0107%	0.0681	4.7
0.6	105.1271	105.2097	0.0786%	0.0683	4.7
0.7	105.1271	105.0324	-0.0901%	0.0679	4.7
0.8	105.1271	105.0773	-0.0474%	0.0681	4.6
0.9	105.1271	105.0625	-0.0615%	0.0680	4.5
1.0	105.1271	105.1125	-0.0139%	0.0678	4.5

Intuitively, incorporating cojumps could be important for more accurately pricing options, as many works from financial time series data have already provided sufficient evidences as referred early in the introduction. The focus of our paper is to propose this new framework and design an exact simulation scheme as the first attempt for implementation, and our part of option pricing is merely illustrative. For future research, empirical work for this new framework, such as parameter calibration, out-of-sample forecast and hedging efficiency, can be carried out as Bakshi et al. (1997). It is particularly interesting to infer the risk premium of cojumps from the real data of option prices as well as the underlying prices. Just like the large family of affine processes (Duffie et al., 2000, 2003), our full model version in Definition 2.1 is very general and would be useful for risk management, such as back testing and stress testing, with a limited computing budget. On the other hand, it may be too flexible and possess too many parameters for calibration, so

special cases are suggested to be used for different purposes. Moreover, it may be possible to be extended to a multivariate framework of shot-noise cojumps for modelling contemporaneous jumps across different assets.

## Notes

- Shot-noise processes have already been used as parsimonious stochastic intensity models (i.e. *shot-noise stochastic intensity* models) for event arrivals in finance and insurance, such as corporate defaults in Duffie and Singleton (1999, 2003) and catastrophes in Dassios and Jang (2003).
- In fact, shot-noise process was used by Bookstaber and Pomerantz (1989) for modelling the volatility dynamics. We use it here for the variance dynamics, but we still name it as a shot-noise stochastic volatility (rather than shot-noise stochastic variance).
- This approach has also been recently adopted by Dassios and Zhao (2013, 2017); Dassios et al. (2018); Qu et al. (2021a,b,c) to develop *tailored* algorithms for exactly sampling some important random variables and point processes, such as tempered stable distributions, Hawkes process, point processes with CIR-intensities, Lévy-driven OU processes and Lévy-driven point processes. The basic idea is simple: to exactly simulate a random variable or a stochastic process, we investigate whether it can be decomposed into simpler random variables exactly in law, each of which can be simulated exactly. However, it is only a *generic* principle and does not tell us anything in detail about how to simulate any targeted random variable or stochastic process, and we have to obtain their distributional properties case by case and identify a successful decomposition which is nontrivial.
- In fact, the point process  $N_t^*$  is a *dynamic contagion process* as introduced by Dassios and Zhao (2011).
- $V_t$  is the so-called *gamma-OU process*, since the asymptotic marginal distribution of volatility process is a simple gamma distribution.
- Alternative approaches can be found in the literature. Petrella and Kou (2004) adopted the numerical inversion of Laplace transform. Broadie and Yamamoto (2005) developed a *fast Gaussian transform* for Gaussian models. Feng and Linetsky (2008) developed a *Hilbert transform* approach based on the convolution for general non-Gaussian Lévy models.
- A positive tempered stable distribution can be constructed from a one-sided  $\alpha$ -stable law by exponential tilting, see (Barndorff-Nielsen and Shephard, 2001b, p.3) and (Barndorff-Nielsen et al., 2002, p.14). It is a popular and basic tool in finance, see some recent applications in Carr et al. (2002), Bates (2012), Li and Linetsky (2013), Mendoza-Arriaga and Linetsky (2014), Todorov (2015) and Andersen et al. (2017). In particular, if  $\alpha = \frac{1}{2}$ , it reduces to a very important distribution, the *inverse Gaussian* (IG) distribution (which can be interpreted as the distribution of the first passage time of a Brownian motion to an absorbing barrier).
- Copula functions are widely used for modelling dependency in finance, insurance and economics, see Embrechts et al. (2002) and Patton (2009) for more details.



## Acknowledgements

The authors would like to thank the reviewer for very helpful and constructive comments and suggestions.

## Funding

The corresponding author Hongbiao Zhao would like to acknowledge the financial support from the National Natural Science Foundation of China (#71401147) and the research fund provided by the Innovative Research Team of Shanghai University of Finance and Economics (#2020110930) and Shanghai Institute of International Finance and Economics.

## ORCID

Hongbiao Zhao  <http://orcid.org/0000-0002-1698-8434>

## References

- Aït-Sahalia, Y., & Hurd, T. R. (2015). Portfolio choice in markets with contagion. *Journal of Financial Econometrics*, 14(1), 1–28. <https://doi.org/10.1093/jfif-nec/nbv024>
- Aït-Sahalia, Y., & Jacod, J. (2014). *High-frequency financial econometrics*. Princeton University Press.
- Aït-Sahalia, Y., Cacho-Diaz, J., & Laeven, R. J. (2015). Modeling financial contagion using mutually exciting jump processes. *Journal of Financial Economics*, 117(3), 585–606. <https://doi.org/10.1016/j.jfineco.2015.03.002>
- Aït-Sahalia, Y., Laeven, R. J., & Pelizzon, L. (2014). Mutual excitation in Eurozone sovereign CDS. *Journal of Econometrics*, 183(2), 151–167. <https://doi.org/10.1016/j.jeconom.2014.05.006>
- Andersen, T. G., Fusari, N., & Todorov, V. (2015a). Parametric inference and dynamic state recovery from option panels. *Econometrica*, 83(3), 1081–1145. <https://doi.org/10.3982/ECTA10719>
- Andersen, T. G., Fusari, N., & Todorov, V. (2015b). The risk premia embedded in index options. *Journal of Financial Economics*, 117(3), 558–584. <https://doi.org/10.1016/j.jfineco.2015.06.005>
- Andersen, T. G., Fusari, N., & Todorov, V. (2017). Short-term market risks implied by weekly options. *The Journal of Finance*, 72(3), 1335–1386. <https://doi.org/10.1111/jofi.12486>
- Asmussen, S., & Glynn, P. W. (2007). *Stochastic simulation: Algorithms and analysis*. Springer.
- Bakshi, G., Cao, C., & Chen, Z. (1997). Empirical performance of alternative option pricing models. *The Journal of Finance*, 52(5), 2003–2049. <https://doi.org/10.1111/j.1540-6261.1997.tb02749.x>
- Baldeaux, J. (2012). Exact simulation of the 3/2 model. *International Journal of Theoretical and Applied Finance*, 15(5), 1250032–1250013. <https://doi.org/10.1142/S021902491250032X>
- Bandi, F. M., & Renò, R. (2012). Time-varying leverage effects. *Journal of Econometrics*, 169(1), 94–113. <https://doi.org/10.1016/j.jeconom.2012.01.010>
- Bandi, F. M., & Renò, R. (2016). Price and volatility co-jumps. *Journal of Financial Economics*, 119(1), 107–146. <https://doi.org/10.1016/j.jfineco.2015.05.007>
- Barndorff-Nielsen, O. E., & Shephard, N. (2001a). Non-Gaussian Ornstein-Uhlenbeck-based models and some of their uses in financial economics. *Journal of the Royal Statistical Society: Series B (Statistical Methodology)*, 63(2), 167–241. <https://doi.org/10.1111/1467-9868.00282>
- Barndorff-Nielsen, O. E., & Shephard, N. (2001b). Normal modified stable processes. *Theory of Probability and Mathematical Statistics*, 65, 1–19.
- Barndorff-Nielsen, O. E., & Shephard, N. (2002). Econometric analysis of realized volatility and its use in estimating stochastic volatility models. *Journal of the Royal Statistical Society: Series B (Statistical Methodology)*, 64(2), 253–280. <https://doi.org/10.1111/1467-9868.00336>
- Barndorff-Nielsen, O. E., Nicolato, E., & Shephard, N. (2002). Some recent developments in stochastic volatility modelling. *Quantitative Finance*, 2(1), 11–23. <https://doi.org/10.1088/1469-7688/2/1/301>
- Bates, D. S. (2000). Post-'87 crash fears in the S&P 500 futures option market. *Journal of Econometrics*, 94(1–2), 181–238. [https://doi.org/10.1016/S0304-4076\(99\)00021-4](https://doi.org/10.1016/S0304-4076(99)00021-4)
- Bates, D. S. (2012). U.S. stock market crash risk, 1926–2010. *Journal of Financial Economics*, 105(2), 229–259. <https://doi.org/10.1016/j.jfineco.2012.03.004>
- Beskos, A., & Roberts, G. O. (2005). Exact simulation of diffusions. *Annals of Applied Probability*, 15(4), 2422–2444.
- Black, F., & Scholes, M. (1973). The pricing of options and corporate liabilities. *Journal of Political Economy*, 81(3), 637–654. <https://doi.org/10.1086/260062>
- Bookstaber, R. M., & Pomerantz, S. (1989). An information-based model of market volatility. *Financial Analysts Journal*, 45(6), 37–46. <https://doi.org/10.2469/faj.v45.n6.37>
- Boswijk, H. P., Laeven, R. J., & Yang, X. (2018). Testing for self-excitation in jumps. *Journal of Econometrics*, 203(2), 256–266. <https://doi.org/10.1016/j.jeconom.2017.11.007>
- Broadie, M., & Kaya, Ö. (2006). Exact simulation of stochastic volatility and other affine jump diffusion processes. *Operations Research*, 54(2), 217–231. <https://doi.org/10.1287/opre.1050.0247>
- Broadie, M., & Yamamoto, Y. (2005). A double-exponential fast Gauss transform algorithm for pricing discrete path-dependent options. *Operations Research*, 53(5), 764–779. <https://doi.org/10.1287/opre.1050.0219>
- Broadie, M., Chernov, M., & Johannes, M. (2007). Model specification and risk premia: Evidence from futures options. *The Journal of Finance*, 62(3), 1453–1490. <https://doi.org/10.1111/j.1540-6261.2007.01241.x>
- Cai, N., Song, Y., & Chen, N. (2017). Exact simulation of the SABR model. *Operations Research*, 65(4), 931–951. <https://doi.org/10.1287/opre.2017.1617>
- Campbell, J. Y., Lo, A. W.-C., & MacKinlay, A. C. (1997). *The econometrics of financial markets*. Princeton University Press.
- Carr, P., & Wu, L. (2017). Leverage effect, volatility feedback, and self-exciting market disruptions. *Journal of Financial and Quantitative Analysis*, 52(5), 2119–2156. <https://doi.org/10.1017/S0022109017000564>
- Carr, P., Geman, H., Madan, D. B., & Yor, M. (2002). The fine structure of asset returns: An empirical investigation. *The Journal of Business*, 75(2), 305–333. <https://doi.org/10.1086/338705>

- Chen, N., & Huang, Z. (2013). Localization and exact simulation of Brownian motion-driven stochastic differential equations. *Mathematics of Operations Research*, 38(3), 591–616. <https://doi.org/10.1287/moor.2013.0585>
- Corradi, V., Silvapulle, M. J., & Swanson, N. R. (2018). Testing for jumps and jump intensity path dependence. *Journal of Econometrics*, 204(2), 248–267. <https://doi.org/10.1016/j.jeconom.2018.02.004>
- Cox, D. R., & Isham, V. (1980). *Point processes*. Chapman and Hall.
- Dassios, A., & Jang, J. (2003). Pricing of catastrophe reinsurance and derivatives using the Cox process with shot noise intensity. *Finance and Stochastics*, 7(1), 73–95. <https://doi.org/10.1007/s007800200079>
- Dassios, A., & Zhao, H. (2011). A dynamic contagion process. *Advances in Applied Probability*, 43(3), 814–846. <https://doi.org/10.1239/aap/1316792671>
- Dassios, A., & Zhao, H. (2013). Exact simulation of Hawkes process with exponentially decaying intensity. *Electronic Communications in Probability*, 18, 1–13. <https://doi.org/10.1214/ECP.v18-2717>
- Dassios, A., & Zhao, H. (2017). Efficient simulation of clustering jumps with CIR intensity. *Operations Research*, 65(6), 1494–1515. <https://doi.org/10.1287/opre.2017.1640>
- Dassios, A., Qu, Y., & Zhao, H. (2018). Exact simulation for a class of tempered stable and related distributions. *ACM Transactions on Modeling and Computer Simulation*, 28(3), 1–20:21. <https://doi.org/10.1145/3184453>
- Duffie, D., & Glynn, P. (1995). Efficient Monte Carlo simulation of security prices. *Annals of Applied Probability*, 5(4), 897–905.
- Duffie, D., & Singleton, K. (1999). *Simulating correlated defaults*. Working paper Stanford University.
- Duffie, D., & Singleton, K. J. (2003). *Credit risk: Pricing, measurement, and management*. Princeton University Press.
- Duffie, D., Filipovic, D., & Schachermayer, W. (2003). Affine processes and applications in finance. *Annals of Applied Probability*, 13(3), 984–1053.
- Duffie, D., Pan, J., & Singleton, K. (2000). Transform analysis and asset pricing for affine jump-diffusions. *Econometrica*, 68(6), 1343–1376. <https://doi.org/10.1111/1468-0262.00164>
- Dungey, M., Erdemlioglu, D., Matei, M., & Yang, X. (2018). Testing for mutually exciting jumps and financial flights in high frequency data. *Journal of Econometrics*, 202(1), 18–44. <https://doi.org/10.1016/j.jeconom.2017.09.002>
- Embrechts, P., McNeil, A., & Straumann, D. (2002). Correlation and dependence in risk management: Properties and pitfalls. In M. A. H. Dempster (Ed.), *Risk management: Value at risk and beyond* (pp. 176–223). Cambridge University Press.
- Eraker, B. (2004). Do stock prices and volatility jump? reconciling evidence from spot and option prices. *The Journal of Finance*, 59(3), 1367–1404. <https://doi.org/10.1111/j.1540-6261.2004.00666.x>
- Eraker, B., Johannes, M., & Polson, N. (2003). The impact of jumps in volatility and returns. *The Journal of Finance*, 58(3), 1269–1300. <https://doi.org/10.1111/1540-6261.00566>
- Feng, L., & Linetsky, V. (2008). Pricing discretely monitored barrier options and defaultable bonds in Lévy process models: A fast Hilbert transform approach. *Mathematical Finance*, 18(3), 337–384. <https://doi.org/10.1111/j.1467-9965.2008.00338.x>
- Fulop, A., Li, J., & Yu, J. (2015). Self-exciting jumps, learning, and asset pricing implications. *Review of Financial Studies*, 28(3), 876–912. <https://doi.org/10.1093/rfs/hhu078>
- Glasserman, P. (2003). *Monte Carlo methods in financial engineering*. Springer.
- Grasselli, M. (2017). The 4/2 stochastic volatility model: A unified approach for the Heston and the 3/2 model. *Mathematical Finance*, 27(4), 1013–1034. <https://doi.org/10.1111/mafi.12124>
- Hawkes, A. G. (1971). Point spectra of some mutually exciting point processes. *Journal of the Royal Statistical Society. Series B (Methodological)*, 33(3), 438–443. <https://doi.org/10.1111/j.2517-6161.1971.tb01530.x>
- Heston, S. L. (1993). A closed-form solution for options with stochastic volatility with applications to bond and currency options. *Review of Financial Studies*, 6(2), 327–343. <https://doi.org/10.1093/rfs/6.2.327>
- Jacod, J., & Todorov, V. (2010). Do price and volatility jump together? *Annals of Applied Probability*, 20(4), 1425–1469.
- Jacod, J., Klüppelberg, C., & Müller, G. (2012). Functional relationships between price and volatility jumps and their consequences for discretely observed data. *Journal of Applied Probability*, 49(4), 901–914. <https://doi.org/10.1239/jap/1354716647>
- Jacod, J., Klüppelberg, C., & Müller, G. (2017). Testing for non-correlation between price and volatility jumps. *Journal of Econometrics*, 197(2), 284–297. <https://doi.org/10.1016/j.jeconom.2016.11.007>
- Kang, C., Kang, W., & Lee, J. M. (2017). Exact simulation of the Wishart multidimensional stochastic volatility model. *Operations Research*, 65(5), 1190–1206. <https://doi.org/10.1287/opre.2017.1636>
- Kou, S. G. (2002). A jump-diffusion model for option pricing. *Management Science*, 48(8), 1086–1101. <https://doi.org/10.1287/mnsc.48.8.1086.166>
- Li, C., & Wu, L. (2019). Exact simulation of the Ornstein–Uhlenbeck driven stochastic volatility model. *European Journal of Operational Research*, 275(2), 768–779. <https://doi.org/10.1016/j.ejor.2018.11.057>
- Li, L., & Linetsky, V. (2013). Optimal stopping and early exercise: An eigenfunction expansion approach. *Operations Research*, 61(3), 625–643. <https://doi.org/10.1287/opre.2013.1167>
- Mendoza-Arriaga, R., & Linetsky, V. (2014). Time-changed CIR default intensities with two-sided mean-reverting jumps. *Annals of Applied Probability*, 24(2), 811–856.
- Merton, R. C. (1976). Option pricing when underlying stock returns are discontinuous. *Journal of Financial Economics*, 3(1–2), 125–144. [https://doi.org/10.1016/0304-405X\(76\)90022-2](https://doi.org/10.1016/0304-405X(76)90022-2)
- Nyström, K., & Zhang, C. (2021). Hawkes-based models for high frequency financial data. *Journal of the Operational Research Society*, 1–18. <https://doi.org/10.1080/01605682.2021.1952116>
- Pan, J. (2002). The jump-risk premia implicit in options: Evidence from an integrated time-series study. *Journal of Financial Economics*, 63(1), 3–50. [https://doi.org/10.1016/S0304-405X\(01\)00088-5](https://doi.org/10.1016/S0304-405X(01)00088-5)
- Patton, A. J. (2009). Copula-based models for financial time series. In T. Mikosch, J.-P. Kreiß, R. A. Davis, & T. G. Andersen (Eds.), *Handbook of financial time series* (pp. 767–785). Springer.

Peng, L., & Xiong, W. (2003). *Time to digest and volatility dynamics*. Working paper Duke University and Princeton University.

Petrella, G., & Kou, S. (2004). Numerical pricing of discrete barrier and lookback options via Laplace transforms. *The Journal of Computational Finance*, 8(1), 1–38. <https://doi.org/10.21314/JCF.2004.114>

Qu, Y., Dassios, A., & Zhao, H. (2021a). Exact simulation of gamma-driven Ornstein-Uhlenbeck processes with finite and infinite activity jumps. *Journal of the Operational Research Society*, 72(2), 471–484. <https://doi.org/10.1080/01605682.2019.1657368>

Qu, Y., Dassios, A., & Zhao, H. (2021b). Exact simulation of Ornstein-Uhlenbeck tempered stable processes. *Journal of Applied Probability*, 58(2), 347–371. <https://doi.org/10.1017/jpr.2020.92>

Qu, Y., Dassios, A., & Zhao, H. (2021c). Random variate generation for exponential and gamma tilted stable distributions. *ACM Transactions on Modeling and Computer Simulation*, 31(4), 1–21. forthcoming. <https://doi.org/10.1145/3449357>

Roberts, G. O., Papaspiliopoulos, O., & Dellaportas, P. (2004). Bayesian inference for non-Gaussian Ornstein-Uhlenbeck stochastic volatility processes. *Journal of the Royal Statistical Society: Series B (Statistical Methodology)*, 66(2), 369–393. <https://doi.org/10.1111/j.1369-7412.2004.05139.x>

Ross, S. A. (1989). Information and volatility: The no-arbitrage martingale approach to timing and resolution irrelevancy. *The Journal of Finance*, 44(1), 1–17. <https://doi.org/10.1111/j.1540-6261.1989.tb02401.x>

Shephard, N. (2005). *Stochastic volatility: Selected readings*. Oxford University Press.

Todorov, V. (2015). Jump activity estimation for pure-jump semimartingales via self-normalized statistics. *Annals of Statistics*, 43(4), 1831–1864.

Todorov, V., & Tauchen, G. (2011). Volatility jumps. *Journal of Business & Economic Statistics*, 29(3), 356–371. <https://doi.org/10.1198/jbes.2010.08342>

Todorov, V., Tauchen, G., & Gryniv, I. (2014). Volatility activity: Specification and estimation. *Journal of Econometrics*, 178(Part 1), 180–193. <https://doi.org/10.1016/j.jeconom.2013.08.015>

Xiu, D. (2014). Hermite polynomial based expansion of European option prices. *Journal of Econometrics*, 179(2), 158–177. <https://doi.org/10.1016/j.jeconom.2014.01.003>

## Appendices

### A. Proof for Theorem 3.1

**Proof.** Changing variable (3.7), the generator of process  $(Z_t, V_t, t)$  acting on any function  $f(z, v, t)$  is

$$\begin{aligned} \mathcal{A}f(z, v, t) &= \frac{\partial f}{\partial t} - \frac{\partial f}{\partial z}(\delta v - \delta v) - \delta v \frac{\partial f}{\partial v} \\ &\quad + \varrho \left[ \int_0^\infty f(z + y, v + y, t) dH(y) - f(z, v, t) \right] \\ &= \frac{\partial f}{\partial t} - \delta v \frac{\partial f}{\partial v} + \varrho \left[ \int_0^\infty f(z + y, v + y, t) dH(y) - f(z, v, t) \right]. \end{aligned}$$

We can find a martingale  $f(Z_t, V_t, t)$  when  $\mathcal{A}f(z, v, t) = 0$ .

Let us set  $\mathcal{A}f(z, v, t) = 0$  and try the solution of form  $e^{-k_1 z} e^{-A(t)v} e^{R(t)}$ , we then get

$$-vA'(t) + R'(t) + \delta vA(t) + \varrho [\hat{h}(k_1 + A(t)) - 1] = 0.$$

Solving the ODE above, we have

$$\begin{aligned} A(t) &= \zeta e^{-\delta t}, \\ R(t) &= \exp \left( \varrho \int_0^t [1 - \hat{h}(k_1 + A(s))] ds \right), \end{aligned}$$

where  $\zeta$  is an arbitrary constant. Let  $k_2 = \zeta e^{-\delta T}$ , then,

$$e^{-k_1 Z_t} e^{-k_2 e^{-\delta(T-t)} V_t} \times \exp \left( \varrho \int_0^t [1 - \hat{h}(k_1 + k_2 e^{-\delta(T-s)})] ds \right)$$

is a martingale. Hence, we obtain the joint Laplace transform of  $(Z_{T+\tau}, V_{T+\tau})$  in (3.6).  $\square$

### B. Proof for Proposition 3.2

**Proof.** Note that, the marginal distribution of  $V_t^*$  is independent of the decay rate  $\delta$  (Barndorff-Nielsen & Shephard, 2001a), so we solve the Laplace transform  $\hat{h}(u)$  in our shot-noise SV model such that its marginal distribution (3.9) is the exactly same as the one from the BNS' SV process  $V_t^*$  with Laplace exponent  $\Phi^*$  and Lévy measure  $\nu^*$ , i.e.

$$\hat{\Pi}(\zeta) = \mathbb{E}[e^{-\zeta V_t^*}],$$

and we have

$$\exp \left( -\frac{\varrho}{\delta} \int_0^\zeta \frac{1 - \hat{h}(u)}{u} du \right) = e^{-\Phi^*(\zeta)},$$

and

$$\Phi^*(\zeta) = \frac{\varrho}{\delta} \int_0^\zeta \frac{1 - \hat{h}(u)}{u} du.$$

Note that,

$$\begin{aligned} \int_0^\infty (1 - e^{-\zeta y}) \nu^*(dy) &= \frac{\varrho}{\delta} \int_0^\zeta \frac{1 - \hat{h}(u)}{u} du \\ &= \frac{\varrho}{\delta} \int_{u=0}^\zeta \frac{1}{u} \int_{y=0}^\infty (1 - e^{-uy}) dH(y) du \\ &= \frac{\varrho}{\delta} \int_{x=0}^\infty (1 - e^{-\zeta x}) \frac{1}{x} \int_{y=x}^\infty dH(y) dx \\ &= \frac{\varrho}{\delta} \int_{x=0}^\infty (1 - e^{-\zeta x}) \frac{1 - H(x)}{x} dx, \end{aligned}$$

then, we have the Lévy measure  $\nu^*$  specified by

$$\nu^*(dy) = \frac{\varrho}{\delta} \frac{1 - H(y)}{y} dy,$$

or, the CDF of volatility-jump sizes, (3.12).  $\square$